Chapter 6

Calibration Hardware for Single-Phase

6.1 Introduction

A detailed understanding of the overall detector response is essential for achieving Deep Underground Neutrino Experiment (DUNE) physics goals. The precision with which each calibration parameter must be measured is spanned by the requirements on the systematic uncertainties for the long-baseline (LBL) and supernova neutrino burst (SNB) physics programs at DUNE. The calibration program must generally provide measurements at the few-percent-or-better level stably across an enormous volume and over a long period and provide sufficient redundancy. This chapter focuses on describing the dedicated calibration hardware systems to be deployed for the DUNE SP module that provide necessary information beyond the reach of external measurements and existing sources and monitors.

A detailed description of the calibration strategy for the DUNE far detector (FD) is provided in Volume II, DUNE Physics, Chapter 4 of this technical design report (TDR). In brief, the calibration strategy uses existing sources of particles, external measurements, and dedicated external calibration hardware systems. Existing calibration sources for DUNE include beam or atmospheric neutrino-induced samples, cosmic rays, argon isotopes, and instrumentation devices such as liquid argon (LAr) purity and temperature monitors. Dedicated calibration hardware systems consist of laser and neutron source deployment systems. External measurements by ProtoDUNE-2 and Short-Baseline Neutrino (SBN) experiments will validate techniques, tools, and the design of systems applicable to the DUNE calibration program. These sources and systems provide measurements of the detector response model parameters, or provide tests of the response model itself. Calibration measurements can also provide corrections to data, data-driven efficiencies, systematics, and particle responses.

The dedicated calibration hardware systems for the SP module include an ionization laser system, a photoelectron laser system, and a pulsed neutron source system. The possibility of deploying a radioactive source system is also currently being explored. The responsibility of the calibration hardware systems falls under the joint single-phase (SP) and dual-phase (DP) calibration

consortium, which was formed in November 2018.

Section 6.2 discusses general aspects driving the calibration program: scope, requirements and data taking strategy. The baseline calibration hardware designs are described in Section 6.3 and respective subsections.

Section 6.3.2 describes the baseline design for the ionization laser system that provides an independent, fine-grained measurement of the electric field throughout the detector, which is an essential parameter that affects the spatial and energy resolution of physics signals. Volume II, DUNE Physics, of this TDR assumes that the fiducial volume (FV) is known to the 1 % level. Through measurements of the spatial distortions and drift velocity map, the laser calibration system mainly helps define the detector FV, thus allowing for the correct prediction of the FD spectra. The laser system also offers many secondary uses such as alignment checks, stability monitoring, and diagnosing detector performance issues. Possible electron lifetime measurements are under study. With the goal of knowing precisely the direction of the laser beam tracks, an independent laser beam location system (LBLS) is also planned, and is described in Section 6.3.3. Alternative designs for the ionization laser system that may improve the physics capability and/or reduce overall cost are also under development and are described in Appendix, Section 6.7.1. Section 6.3.4 describes the photoelectron laser system that can be used to rapidly diagnose electronics or time projection chamber (TPC) response issues along with many other useful measurements such as integrated field across drift, drift velocity, and electronics gain.

Section 6.3.5 describes the baseline design for the pulsed neutron source (PNS) system, which provides a triggered, well defined, energy deposition from neutron capture in Ar detectable throughout the detector volume. Neutron capture is an important component of signal processes for SNB and LBL physics, enabling direct testing of the detector response spatially and temporally for the low-energy program and the efficiency of the detector in reconstructing the low-energy spectra. A spatially fine-grained measurement of electron lifetime is also planned with this source. The proposed radioactive source deployment system (RSDS) described in the Appendix, Section 6.7.3, is in many ways complementary to the PNS system, and can provide at known locations inside the detector a source of gamma rays in the same energy range of SNB and solar neutrino physics. The RSDS is the only calibration system that could probe the detection capability for single isolated solar neutrino events and study how well radiological backgrounds can be suppressed. In contrast, the PNS is externally triggered and does not provide such a well defined source location for gamma rays inside the detector. On the other hand, the PNS can probe the uniformity of the full detector, while the RSDS could only scan the ends of the detector.

For all the calibration hardware systems, the goal is to deploy prototype designs and validate them at ProtoDUNE-2 during the post long shutdown 2 (LS2) running at European Organization for Nuclear Research (CERN). The validation plan for calibration systems at ProtoDUNE-2 and other experiments is described in Section 6.3.6.

Section 6.4 describes interfaces calibration has with other DUNE consortia, especially with data acquisition (DAQ) which are described in more detail in Section 6.4.1.

Sections 6.5 and 6.6 conclude the chapter with descriptions of the aspects related to construction and installation of the systems, as well as organizational aspects, including schedule and milestones,

discussed in Section 6.6.4.

6.2 Calibration Overview

This section focuses on the general aspects of calibrations in DUNE: the scope of the consortium activities and planned systems; the physics and performance requirements driving the design; and the overall strategy for usage of the systems, in combination with natural sources.

6.2.1 Scope

The scope of the calibration consortium includes a laser ionization system, a photoelectron laser system, a laser beam location system, and a pulsed neutron source system. In addition, the consortium is evaluating a radioactive source deployment system. The calibration consortium is responsible for design through commissioning in the SP module for these calibration devices and their associated feedthroughs. Validating the designs of calibration systems at ProtoDUNE-2 (and other experiments as relevant) is also included under the scope of the consortium. Figure 6.1 shows the subsystems included under the calibration consortium.

Chapters 3, 4, 5, and 8 of Volume IV, The DUNE Far Detector Single-Phase Technology, of this TDR describe other hardware essential for calibration such as cold electronics (CE) external charge injection systems, high voltage (HV) monitoring devices, photon detection system (PD system) stability monitoring devices, and cryogenics instrumentation and detector monitoring devices, respectively. The scope of these systems is described by their respective consortia, and the calibration consortium has substantial interfaces with these consortia. The use of other calibration sources such as external measurements and existing sources of particles (e.g., muons, pions) is discussed in the calibration section of TDR Volume II, DUNE Physics, Chapter 4.

We are pursuing the effects of calibration on physics and related studies. Calibrations also require simulations (e.g., E field) to identify desirable locations for calibration devices in the cryostat, away from regions of high E field, so that their presence does not induce large field distortions. The design of the calibration systems and understanding the related physics requires coordination with other consortia and groups. This is discussed in Section 6.4.

6.2.2 Design Considerations and Requirements

Some common design considerations for calibration devices include stability, reliability, and longevity, so calibration systems can be operated for the lifetime of the experiment (20 years). Such longevity is uncommon for any device, so the overall design permits replacing devices where possible, namely the parts that are external to the cryostat. The systems must also adhere to relevant global requirements of the DUNE detector. Table 6.1 shows the top-level overall requirements for calibration

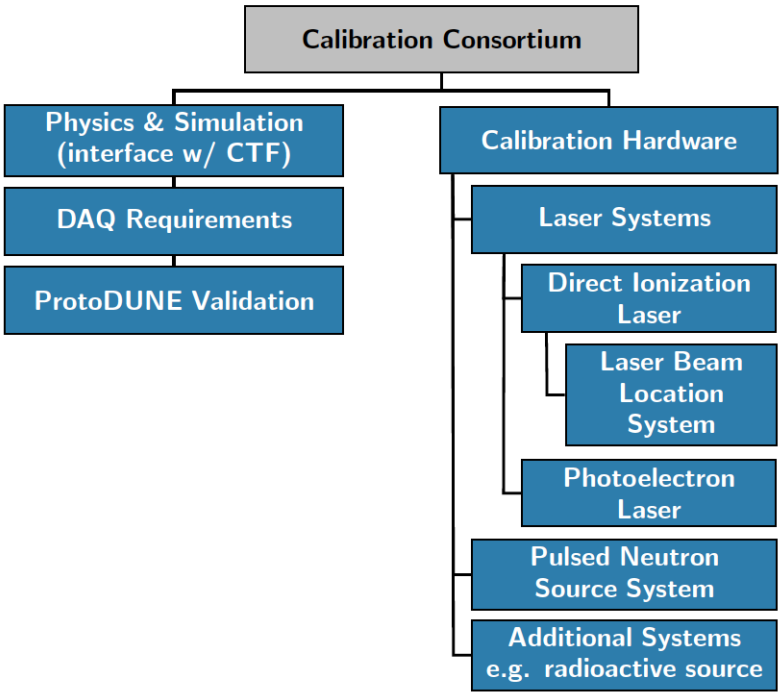

Figure 6.1: Calibration consortium subsystem chart. CTF stands for Calibration Task Force.

subsystems along with global DUNE requirements that are relevant for calibration. For example, DUNE requires the E field on any instrumentation device inside the cryostat to be less than 30 kV/cm to minimize the risk of dielectric breakdown in LAr. Another consideration important for event reconstruction is understanding the maximum tolerable level of noise on the readout electronics due to calibration devices and implementing proper grounding schemes to minimize it. ProtoDUNE-SP is evaluating this. In Table 6.1, two values are quoted for most of the parameters: 1) specification, which is the minimum requirement to guarantee baseline performance, and 2) goal, an ideal requirement for achieving improved precision.

For the ionization laser system, the energy and position reconstruction requirements for physics measurements lead to requirements for the necessary precision in measuring the TPC E field as well as its spatial coverage and granularity. The precision of the E field measurement with the laser system must be about 1 % so that the effect from E field on the collected charge, via the dependence of the recombination factor on E field, is well below 1 %. This is also motivated by consistency with the high level DUNE specification of 1 % on field uniformity throughout the volume for component alignment and the HV system. For laser coverage, to keep the E field measurement at the ∼1 % level, we are aiming for a coverage of 75 % or more of the total FV. The requirement on granularity for the laser is estimated based on the FV uncertainty requirements (1 %) and corresponding uncertainty requirements (1.5 cm) in each coordinate. A specification is set for a voxel size of $30\times30\times30\,\mathrm{cm}^3$, that should be sufficient to satisfy the FV uncertainty requirements. A goal is set for $10\times10\times10\,\mathrm{cm}^3$, which could allow for a refinement in precision in some detector regions.

The laser beam location must also meet the level of reconstruction requirement in each coordinate,

approximately 5 mm. In order to reach that over distances of up to 20 m, where the latter is the maximum distance that any beam needs to travel to cover all detector voxels, this results in a stringent alignment requirement of 0.015° (or 0.25 mrad) on the pointing precision. The laser beam location system is also designed to check the beam location with a precision of 5 mm over distances of up 20 m. The data volume for the ionization laser system must be no more than 184 TB/year/10 kt, assuming 800k laser pulses, $10\times10\times10\,\mathrm{cm}^3$ voxel sizes, a 100 µs zero suppression window, and two dedicated calibration campaigns per year.

For the PNS system, the system must provide sufficient neutron event rate to make spatially separated precision measurements across the detector of a comparable size to the voxels probed by the laser ($30\times30\times30\,\mathrm{cm}^3$) for most regions of the detector (75 %). For the SNB program, the sensitivity to distortions of the neutrino energy spectrum depends on the uncertainties in the detection threshold and the reconstructed energy scale and resolution. Studies discussed in the physics TDR present target ranges for the uncertainties in these parameters [96] as a function of energy. The measurements with the PNS system aim to provide response corrections and performance estimates, so those uncertainty targets are met throughout the whole volume. This ensures that each voxel has sufficient neutron event rate (percent level statistical uncertainty).

In terms of data volume requirements, the PNS system requires at least 144 TB/year/10 kt assuming 10^5 neutrons/pulse, 100 neutron captures/m^3, and 130 observed neutron captures per pulse, and two calibration runs per year.

Table 6.2 shows the full set of requirements related to all calibration subsystems. More details on each of the requirements can be found under dedicated subsections.

Table 6.1: Calibration specifications

Label	Description	Specification (Goal)	Rationale	Validation
SP-FD-1	Minimum drift field	> 250 V/cm (> 500 V/cm)	Lessens impacts of e^--Ar recombination, e^- lifetime, e^- diffusion and space charge.	ProtoDUNE
SP-FD-2	System noise	< 1000 e^-	Provides >5:1 S/N on induction planes for pattern recognition and two-track separation.	ProtoDUNE and simulation
SP-FD-5	Liquid argon purity	< 100 ppt (< 30 ppt)	Provides >5:1 S/N on induction planes for pattern recognition and two-track separation.	Purity monitors and cosmic ray tracks
SP-FD-7	Drift field uniformity due to component alignment	< 1 % throughout volume	Maintains APA, CPA, FC orientation and shape.	ProtoDUNE
SP-FD-9	APA wire spacing	4.669 mm for U,V; 4.790 mm for X,G	Enables 100% efficient MIP detection, 1.5 cm yz vertex resolution.	Simulation
SP-FD-11	Drift field uniformity due to HVS	< 1 % throughout volume	High reconstruction efficiency.	ProtoDUNE and simulation
SP-FD-13	Front-end peaking time	1 µs	Vertex resolution; optimized for 5 mm wire spacing.	ProtoDUNE and simulation

SP-FD-22	Data rate to tape	< 30 PB/year	Cost. Bandwidth.	ProtoDUNE
SP-FD-23	Supernova trigger	$>$ 95 % efficiency for a SNB producing at least 60 interactions with a neutrino energy >10 MeV in 12 kt of active detector mass during the first 10 seconds of the burst.	$>$95% efficiency for SNB within 20 kpc	Simulation and bench tests
SP-FD-24	Local electric fields	< 30 kV/cm	Maximize live time; maintain high S/N.	ProtoDUNE
SP-FD-25	Non-FE noise contributions	$<< 1000\ e^-$	High S/N for high reconstruction efficiency.	Engineering calculation and ProtoDUNE
SP-FD-26	LAr impurity contributions from components	$<< 30$ ppt	Maintain HV operating range for high live time fraction.	ProtoDUNE
SP-FD-27	Introduced radioactivity	less than that from ^{39}Ar	Maintain low radiological backgrounds for SNB searches.	ProtoDUNE and assays during construction
SP-FD-29	Detector uptime	$>$98% ($>$99%)	Meet physics goals in timely fashion.	ProtoDUNE
SP-FD-30	Individual detector module uptime	$>$90% ($>$95%)	Meet physics goals in timely fashion.	ProtoDUNE
SP-CALIB-1	Ionization laser E field measurement precision	1 %	E field affects energy and position measurements.	ProtoDUNE and external experiments.
SP-CALIB-2	Ionization laser E field measurement coverage	$>$ 75 % (100 %)	Allowable size of the uncovered detector regions is set by the highest reasonably expected field distortions, 4 %.	ProtoDUNE
SP-CALIB-3	Ionization laser E field measurement granularity	$30 \times 30 \times 30$ cm^3 ($10 \times 10 \times 10$ cm^3)	Minimum measurable region is set by the maximum expected distortion and position reconstruction requirements.	ProtoDUNE
SP-CALIB-4	Laser beam location precision	0.5 mrad ($<$ 0.5 mrad)	The necessary spatial precision does not need to be smaller than the APA wire gap.	ProtoDUNE
SP-CALIB-5	Neutron source coverage	$>$ 75 % (100 %)	Set by the energy resolution requirements at low energy.	Simulations
SP-CALIB-6	Ionization laser data volume per year (per 10 kt)	$>$ 184 TB/yr/10kt ($>$ 368 TB/yr/10kt)	The laser data volume must allow the needed coverage and granularity.	ProtoDUNE and simulations
SP-CALIB-7	Neutron source data volume per year (per 10 kt)	$>$ 144 TB/yr/10kt ($>$ 288 TB/yr/10kt)	The pulsed neutron system must allow the needed coverage and granularity.	Simulations

Table 6.2: Full list of Specifications for the Calibration Subsystems.

Quantity/Parameter	Specification	Goal
Noise from calibration devices	$\ll$ 1000 enc	
Max. E field near calibration devices	$<$ 30 kV/cm	$<$15 kV/cm
Direct Ionization Laser System		
E field measurement precision	1%	$<$1%
E field measurement coverage	$>$ 75%	100%
E field measurement granularity	$<$ 30x30x30 cm	10x10x10 cm
Top field cage penetrations (alternative design)	to achieve desired laser coverage	
Data volume per 10 kton	184 TB/year	368 TB/year
Longevity, internal parts	20 years	$>$ 20 years
Longevity, external parts	5 years	$>$ 20 years
Laser Beam Location System		
Laser beam location precision	0.5 mrad	0.5 mrad
Longevity	20 years	$>$ 20 years
Photoelectron Laser System		
Longevity, internal parts	20 years	$>$ 20 years
Longevity, external parts	5 years	$>$ 20 years
Pulsed Neutron Source System		
Coverage	$>$ 75%	100%
Data volume per 10 kton	144 TB/year	288 TB/year
Longevity	3 years	$>$ 20 years

6.2.3 Strategy

Once the far detector is filled and at the desired high voltage, it immediately becomes live for all non-beam physics signals, so it is important to tune the detector response model with calibration data as early as possible. Moreover, since both beam and non-beam physics data will have a fairly uniform rate, regular calibrations in order to monitor space and time dependencies are also needed.

Following those considerations, the strategy for calibration data taking will be organized around three specific periods:

Commissioning As soon as the detector is full, with HV on and the DAQ operational, it is useful to take laser calibration data. The main goal is to help identify problems in the anode plane assembly (APA) wires or the electronics channels, or large cool-down distortions. Depending on how long the ramp-up will take, it could be useful to take data before the HV reaches the nominal level, because we can identify problems earlier and possibly learn about dependency of various detector parameters with E field.

Early data During the early stages of data-taking, the goal is to do the fullest possible fine-grained laser and neutron calibration (E field map, lifetime, low energy scale/resolution response) as early as possible, so that all the physics can benefit from a calibrated detector from day 1. These results should be combined at a later stage with detector-wide average measurements with cosmics.

Stable data-taking The main goal of calibrations during stable data-taking is to track possible variations of detector response parameters, and contribute to constraining the detector systematics. We expect to combine fine-grained, high statistics scans at regular time intervals – twice a year for laser, six times for the pulsed neutron source – with more frequent coarse-grained scans (e.g., photoelectron laser, large voxel ionization laser scan). These, combined with analysis of cosmic ray and radiological backgrounds data, can alert to the need of additional fine scans in particular regions.

6.3 Calibration Systems

DUNE plans to build two primary systems dedicated to calibrate the SP module – a laser system and a pulsed neutron source system – both of which require interfaces with the cryostat, that are described in Section 6.3.1.

The laser system is aimed at determining the essential detector model parameters with high spatial and time granularity. The primary goal is to provide maps of the drift velocity and E field, following a position-based technique already proven in other liquid argon time-projection chamber (LArTPC) experiments. Two laser sub-systems are planned. With high intensity coherent laser pulses, charge can be created in long straight tracks in the detector by direct ionization of LAr with the laser beams. This is described in Section 6.3.2. An auxiliary system aimed at an independent

measurement and cross-check of the laser track direction is described in Section 6.3.3. On the other hand, laser excitation of targets placed on the cathode creates additional charge from well-defined locations that can be used as a general TPC monitor and to measure the integrated drift time. This is described in Section 6.3.4.

The PNS system provides a "standard candle" neutron capture signal (6.1 MeV multi-gamma cascade) across the entire DUNE volume that is directly relevant to the supernova physics signal characterization thus validating the performance of the detector in the low energy regime. The PNS system is described in detail in Section 6.3.5.

The physics motivation, requirements and design of these systems are described in the following subsections. Alternative designs for the ionization laser system, pulsed neutron source system, as well as the proposed radioactive source deployment system, are described in Sections 6.7.1, 6.7.2, and 6.7.3 of the Appendix, respectively.

6.3.1 Cryostat Configuration for Calibration Systems

Figure 6.2 shows the current cryostat design for the SP module with penetrations for various subsystems. The penetrations dedicated to calibration are the highlighted black circles.

In addition to these dedicated ports, there are plans to use the detector support system (DSS) and cryogenics ports (orange and blue dots in Figure 6.2) as needed to route cables for other calibration systems, e.g., fiber optic cables for the photon detector (PD) calibration system, which is described in Chapter 5. DSS and cryogenics ports can be accommodated by feedthroughs with a CF63 side flange for this purpose.

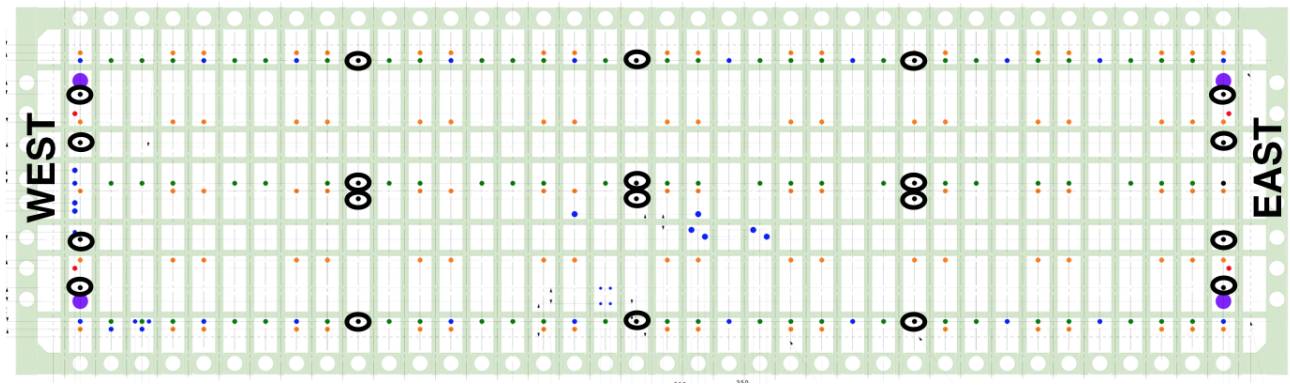

Figure 6.2: Top view of the SP detector module cryostat showing various penetrations. Circles highlighted in black are multi-purpose calibration penetrations. The green dots are TPC signal cable penetrations. The blue ports are cryogenics ports. The orange ports are DSS penetrations. The larger purple ports at the four corners of the cryostat are human access ports.

The current plan is to use the calibration ports for several different purposes, but their placement is largely driven by requirements for the ionization track laser. The ports toward the center of the cryostat are placed near the APAs, where the E field is small, to minimize any risks due to HV discharge. HV is not an issue for the far east and west ports since they are located outside

the field cage (FC) and the penetrations are located close to mid-drift (a location favorable for possible source deployment). Implementing the baseline ionization track laser system as described in Section 6.3.2 requires 12 feedthroughs, the three central ones in each of the four TPC drift volumes; this arrangement allows lasers to be used for full volume calibration of the E field and associated diagnostics (e.g., HV).

The distance between any two consecutive feedthrough columns shown in Figure 6.2 is approximately 15 m. Since the MicroBooNE laser system has shown that tracks will propagate over that detector's full 10 m length, this distance is considered reasonable. Assuming that the effects of Rayleigh scattering and self-focusing (Kerr effect) do not limit the laser track length, this laser arrangement could illuminate the full volume with crossing tracks in the central region, and single tracks in the region closer to the end-walls. At this time, the maximum usable track length is unknown, and it may be that the full 60 m detector module length could be covered by the laser system after optimization.

Throughout this chapter, the following convention for the coordinate axes will be used: x is parallel to the drift direction, y is the vertical, and z is parallel to the beamline. This is illustrated in Chapter 8 Figure 8.3.

6.3.2 Laser Calibration: Ionization System

Through its effect on drift velocity, recombination, and lifetime, the E field is a critical parameter for physics signals as it ultimately affects the spatial resolution and energy response of the detector. The primary purpose of a laser system is to provide an independent, fine-grained estimate of the E field in space and time. It would be extremely valuable to achieve measurements of electron lifetime with the laser system, but the feasibility of that is still under discussion. The R&D plan in ProtoDUNE-2 will address the feasibility of carrying out charge-based measurements which, if successful, would open up the possibility of using the laser to measure electron lifetime. So, except where specifically indicated, the rest of this section will focus on drift velocity and E field measurement.

6.3.2.1 Physics Motivation

Because it measures spatial distortions of straight tracks, the laser system actually measures the local drift velocity field directly and helps define the detector FV, and this in itself is an important input for the LBL analysis. However, it is still important to use information independent of the charge in order to disentangle effects like lifetime and recombination from E field distortions. The laser system can do this, by using the position information to derive the E field from the local velocity map, taking into account the colinearity between both vectors, and the relatively well studied relation between the magnitude of the drift velocity and the E field, considering a temperature dependence (see [97] and references [29, 45-58] therein). A laser system also has the intrinsic advantage of being immune to recombination effects, thus eliminating particle-dependent effects.

Several sources may distort the E field temporally and/or spatially in the detector. Current simulation studies indicate that positive ion accumulation and drift (space charge) due to ionization sources such as cosmic rays or ^{39}Ar is small in the DUNE FD, causing E field distortions of at most 0.1 % [98]. However, not enough is known yet about the fluid flow pattern in the FD to exclude the possibility of stable eddies that may amplify the effect for both SP and DP modules. This effect can be further amplified significantly in the DP module due to accumulation in the liquid of ions created by the electron multiplication process in the gas phase. Additionally, other sources in the detector (especially detector imperfections) can cause E field distortions. For example, FC resistor failures, non-uniform resistivity in the voltage dividers, cathode plane assembly (CPA) misalignment, CPA structural deformations, and APA and CPA offsets and deviations from flatness can create localized E field distortions. These effects are presented in Figures 6.3 and 6.4, showing the effect of a few % on the E field from 2 cm CPA position tilts and up to 4 % from FC single resistor failures.

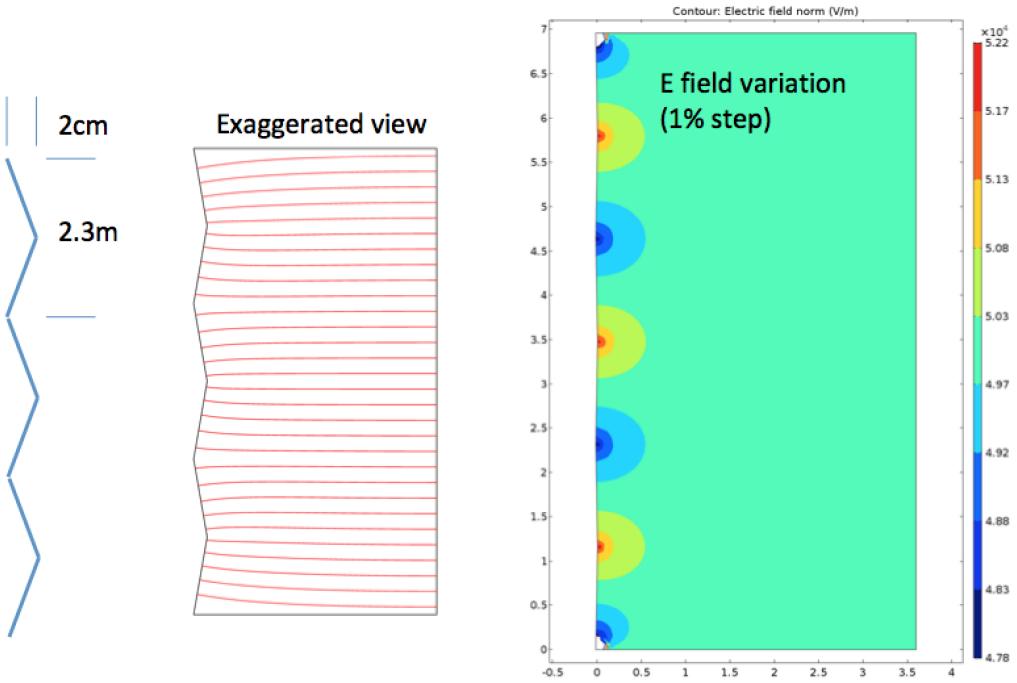

Figure 6.3: Illustration of a possible distortion of the CPA position [99], assuming a 2 cm swing, and its impact on E field (right).

In both SP and DP modules, a resistor failure will create significant, local E field distortions that must be identified. In the DP module, four resistors would have to fail to cause a failure across the FC gap, but even one failure in the SP module can have an effect; this may be partly, but not completely, mitigated by modifying the HV. While the resistor failure will be detected temporally, its location in space is not possible to determine from slow controls monitoring data. Misalignments of detector objects or deformations may also create E field distortions; while individual effects may be small, it is possible to have a combined, significant effect. Each individual E field distortion may add in quadrature with other effects, and can aggregate up to 4 % under certain conditions. Understanding all these effects requires in situ measurement of E field for proper calibration.

Useful secondary uses of laser include alignment (especially modes that are weakly constrained

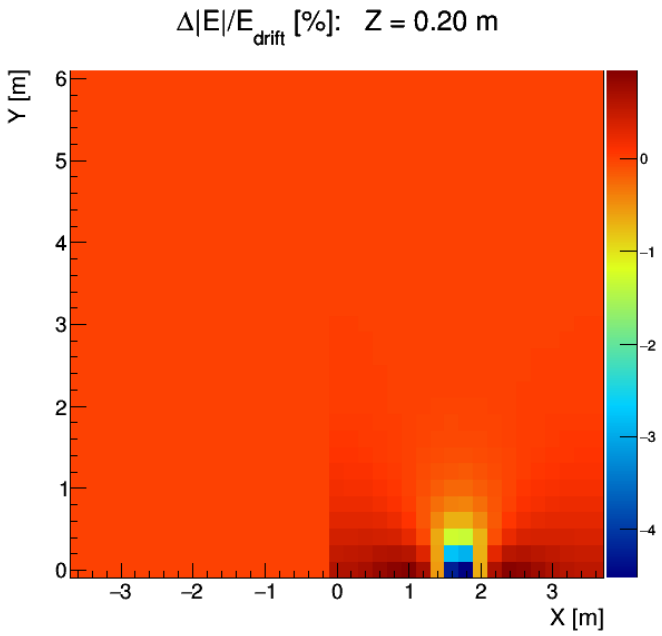

Figure 6.4: Impact on E field magnitude distortions of a single FC resistor failure [100].

by cosmic rays), stability monitoring, and diagnosing detector performance issues (e.g., HV). Misalignment may include physical deformation and/or rotations of objects within the detector. Given the expected low rate of cosmic ray events (about 3500/day/10-kt, inclusive) at the underground location, calibration with cosmic rays is not possible over short time scales. Even over long time scales, certain alignment directions are difficult to assess with cosmic rays alone, such as distortions of the detector that preserve the gap widths and do not shift the APAs in x near the gaps relative to one another. These distortions include global shifts and rotations in the locations of all detector elements, and crumpling modes where the edges of the APAs hold together but angles are slightly different from nominal.

With respect to electron lifetime, the preliminary results from ProtoDUNE-SP purity monitors and cosmic ray analyses indicate significant variations with time and space, both between monitors at different vertical coordinates (see Chapter 8), and between the regions inside and outside the TPC. The possibility of carrying out such measurements with the ionization laser is therefore quite interesting. The ArgonTUBE experiment obtained lifetime measurements with laser [101] compatible with the cosmic ray ones, but it is not clear yet if this is possible at very large scales, since the modelling of the density of ionization charge created along the tracks presents challenges related to the previously mentioned self-focusing. Therefore the characterization of the ionization charge density from laser tracks will be an important goal of the development plan in ProtoDUNE-2.

6.3.2.2 Requirements

The energy and position reconstruction requirements for physics measurements lead to requirements on the necessary precision of the laser E field measurement, its spatial coverage and gran-

ularity. The next sections discuss the rationale behind each requirement, which we take as the DUNE specification.

E field precision: In the LBL and high-energy range, Volume II, DUNE Physics, Chapter 5 of this TDR states that the calibration information must provide approximately 1 to 2 % understanding of normalization, energy scale and resolution, and position resolution within the detector. Because a smaller E field leads to higher electron-ion recombination and therefore a lower collected charge, distortions of the E field can introduce energy scale bias. To connect this to a specification for the necessary precision of the E field measurement, we note that, via recombination studies [98], we expect a 1 % distortion on E field to lead to a 0.3 % bias on collected charge. Because other effects will contribute to the lepton energy scale uncertainty budget, we consider a goal for the laser system to measure the E field to a precision of ∼1 % so that its effect on the collected charge is well below 1 %. This is also motivated by consistency with the high level DUNE specification on field uniformity throughout the volume due to component alignment and HV system, that is set at 1 %. Together with two other high-level DUNE specifications, the APA wire spacing (4.7 mm) and the front end peaking time (1 µs), the effect of this E field precision requirement on engineering parameters of the calibration laser system is discussed further in Section 6.3.2.3.1.

E field measurement coverage: In practice, measuring the E field throughout the whole volume of the TPC will be difficult, so we must establish a goal for the coverage and granularity of the measurement. Until a detailed study of the propagation of the coverage and granularity into a resolution metric is available, a rough estimate of the necessary coverage can be made as follows.

Assuming 4 % as the maximum E field distortion that is expected from a compounding of multiple possible effects in the DUNE FD as described in the previous section, we can then ask what would be the maximum acceptable size of the spatial region uncovered by the calibration system, if a distortion of that magnitude (systematically biased in the same direction) were present in that region. Our criterion of acceptability is to keep the overall E field distortion, averaged over the whole detector, at the 1 % level. To meet this requirement, the aforementioned spatial region should be no larger than 25 % of the total fiducial volume. Therefore, we aim to have a coverage of 75 % or more.

In addition, we need to consider that the method used to estimate E field distortions is based on obtaining position displacement maps [102], and that the comparison between the reconstructed and true direction of a single track does not unambiguously determine a specific displacement map. Having tracks coming from different origins crossing in the same position is a direct way to eliminate that ambiguity, since the displacement vector is given simply by the vector connecting the intersections of the two reconstructed and the two true tracks. A joint iterative analysis of several close-by tracks is the default method for all other positions, but the system design should allow for the maximum possible number of positions for crossing tracks from different beams.

E field measurement granularity: Volume II (DUNE Physics) of this TDR states that a FV uncertainty of 1 % is required. This translates to a position uncertainty of 1.5 cm in each coordinate

(see Chapter 2). In the y and z coordinates, position uncertainty is given mainly by the APA wire pitch, and since this is about 4.7 mm, the requirement is met. In the drift (x) direction, the position is calculated from timing, and considering the electronics peaking time of 1 µs, the uncertainty should be even smaller.

The position uncertainty, however, also depends on the E field, via the drift velocity. Because the position distortions accumulate over the drift path of the electron, it is not enough to specify an uncertainty on the field. We must accompany it by specifying the size of the spatial region of that distortion. For example, a 10 % distortion would not be relevant if it was confined to a 2 cm region and if the rest of the drift region was at nominal field. Therefore, what matters is the product of [size of region] × [distortion]. Moreover, one can distinguish distortions into two types:

1. Those affecting the magnitude of the field. Then the effect on the drift velocity v is also a change of magnitude. According to the function provided in [103], close to $500\,\mathrm{V}\cdot\mathrm{cm}^{-1}$, the variation of the velocity with the field is such that a 4 % variation in field E leads to a 1.5 % variation in v.

2. Those affecting the direction of the field. Nominally, the field E should be along x, so $E = E_L$ (the longitudinal component). If we consider that the distortions introduce a new transverse component E_T, in this case, this translates directly into the same effect in the drift velocity, which gains a v_T component, $v_T = v_L E_T/E_L$, i.e., a 4 % transverse distortion on the field leads to a 4 % transverse distortion on the drift velocity.

Thus, a 1.5 cm shift comes about from a constant 1.5 % distortion in the velocity field over a region of 1 m. In terms of E field, that could be from a 1.5 % distortion in E_T over 1 m or a 4 % distortion in E_L over the same distance.

E field distortions can be caused by space-charge effects due to accumulation of positive ions caused by ^{39}Ar decays (cosmic ray rate is low in FD), or detector defects, such as CPA misalignments (Figure 6.3), FC resistor failures (Figure 6.4), resistivity non-uniformities, etc. These effects added in quadrature can be as high as 4 %. The space charge effects due to ^{39}Ar [98] can be approximately 0.1 % for the single-phase (SP), and 1 % for the DP (dual-phase), so in practice these levels of distortions must cover several meters to be relevant. Other effects due to CPA or FC imperfections can be higher because of space charge, but they are also much more localized. If we assume there are no foreseeable effects that would distort the field more than 4 %, and considering the worst case scenario (transverse distortions), then the smallest region that would produce a 1.5 cm shift is 1.5 cm/0.04 = 37.5 cm. This provides a target for the granularity of the measurement of the E field distortions in x to be smaller than approximately 30 cm, with, of course, a larger region if the distortions are smaller. Given the above considerations, then a voxel size of $10\times10\times10\,\mathrm{cm}^3$ appears to be enough to measure the E field with the granularity needed for a good position reconstruction precision. In fact, because the effects that can likely cause bigger E field distortions are problems or alignments in the CPA (or APA) or in the FC, it is conceivable to have different size voxels for different regions, saving the highest granularity of the probing for the walls/edges of the drift volume.

6.3.2.3 Design

The design of the laser calibration system for DUNE is largely based on the design of the system built for MicroBooNE [4], which in turn was based on several previous developments [104, 105, 106, 107]. A similar system was also built for CAPTAIN [108] and in the near future, will be built for SBND [109]. Operation of the MicroBooNE system has already taken place. A preliminary report was given in [110], and more details on the data analysis are available in [102].

Design overview Ionization of LAr by laser can occur via a multiphoton process in which two-photon absorption [111] leads the atom to the excited states band, and a third photon subsequently causes ionization. This can only occur with high photon fluxes, and so the lasers must provide pulse energies of 60 mJ or more within a few ns. Unlike muons, the laser beams do not suffer multiple scattering and travel along straight lines determined by the steering mirror optics. The basic measurement consists of generating laser ionization tracks in the TPC and comparing the reconstructed tracks with the direction known from the steering hardware. An apparent curvature of the measured track is attributed to drift velocity, and therefore E field, distortions (either in direction or magnitude).

While the Rayleigh scattering length for 266 nm light is approximately 40 m, additional optics effects may limit the maximum practical range of laser beams of that wavelength to a distance smaller than that. Those can include the Kerr effect due to the dependency of the refractive index on the E field. In the presence of an intense field, such as that caused by the laser beam itself, the change in refractive index can lead to lensing, or focusing, that distorts the coherence of the beam[1]. Despite this, laser beams with lengths of 10 m in LAr have been observed in MicroBooNE, and beams with 20 m lengths (possibly more) can be reasonably expected to obtain with a similar system. This has determined the choice of locating five calibration ports in the cryostat roof at 15 m intervals along each of the four drift volumes of the SP module, for a total of 20 ports. In fact, there are four ports just outside each of the FC end-walls, and 12 ports located over the top FC, close to the APA of each drift volume, as shown in Figure 6.2. As is discussed further below, the number of ports currently assigned for the ionization laser system in the baseline design is 12, a compromise between having the maximum possible coverage with crossing tracks and cost considerations.

Mechanical and optical design for a single port sub-system For each of the used calibration ports, a laser sub-system can be schematically represented by Figure 6.5 (left) and consists of the following elements:

- a laser box (see Figure 6.5, right) that provides
  - a Nd:YAG laser, with the fourth harmonic option providing 266 nm in intense 60 mJ

[1] The Kerr effect is so far believed to be the cause of non-homogeneity of the ionization along the laser beam observed in MicroBooNE, which prevents the use of the charge information. Its effect on the position measurement and E field uncertainty has been studied by MicroBooNE.

pulses with about 5 ns width, with a divergence of 0.5 mrad. The Surelite SL I-10 laser[2] is a possible choice since it has been successfully used in the past in other experiments.
  - an attenuator and a collimator to control the intensity and size of the beam;
  - a photodiode that gives a TPC-independent trigger signal;
  - a low-power red laser, aligned with the UV laser, to facilitate alignment operations; and
  - a Faraday cage to shield the surrounding electronics from the accompanying electromagnetic pulse.
- a feedthrough (see Figure 6.6, left) into the cryostat that provides
  - the optical coupling that allows the UV light to pass through into the cryostat directly into the liquid phase, avoiding distortions due to the gas-liquid interface and the gas itself;
  - a rotational coupling that allows the whole structure to rotate while maintaining the cryostat seal;
  - a periscope structure (see Figure 6.6; Right) mounted under the rotating coupling that supports a mirror within the LAr;
  - the additional theta rotation of the mirror accomplished by a precision mechanism coupled to an external linear actuator; and
  - both the rotation and linear movements of the steering mechanism read out by precision encoders.

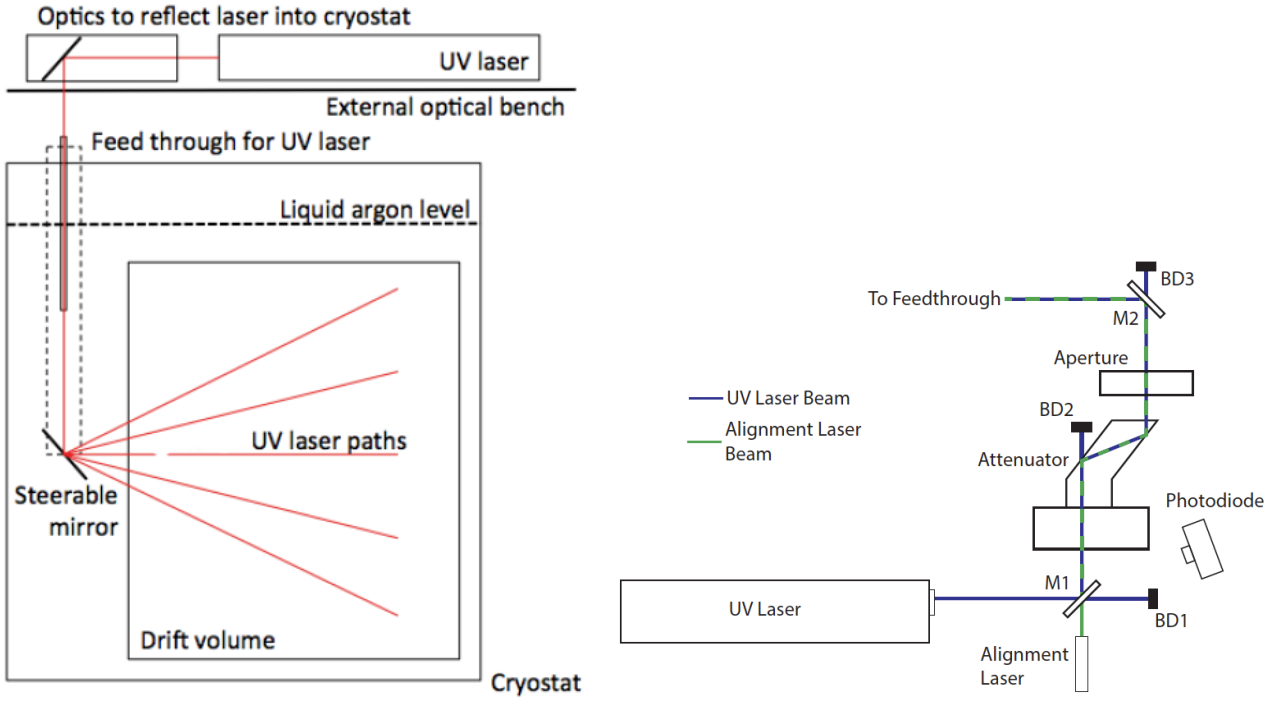

Figure 6.5: Left: Schematics of the ionization laser system in one port [109]. Right: Schematics of the laser box [4].

The goal of the mechanical design of the system is to achieve a precision close to that of the

[2]Amplitude Surelite™ https://amplitude-laser.com/wp-content/uploads/2019/01/Surelite-I-II-III.pdf

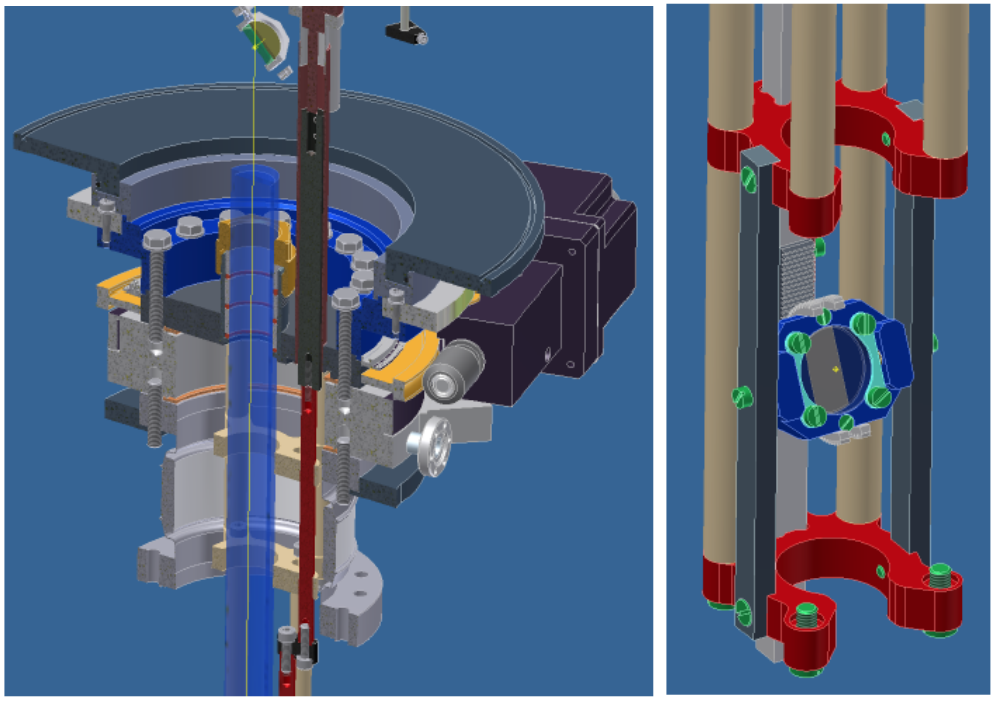

Figure 6.6: CAD drawings of the MicroBooNE laser calibration system [4]. Left: calibration port feedthrough. Right: laser beam periscope.

TPC position measurements, so that no single factor dominates the overall systematics. The TPC precision of about 5 mm in the y, z coordinates is given primarily by the wire spacing of 4.7 mm and 4.8 mm. The precision of about 2 mm on the x coordinate comes essentially from the 1 µs peaking time of the front-end electronics and the typical drift velocity (1.6 mm/µs).

The starting point of the laser beams is given by the position of the mirror in the periscope, which is known from construction drawings, warm surveys and cool down calculations. The angle of the beam is given by the angles (θ, ϕ) of the mirror, which are set by the periscope motors and read out by the encoders. For MicroBooNE, reference [110] quotes a very good 0.05 mrad precision (0.5 mm at 10 m) from the encoders alone, and an overall pointing precision of 2 mm at 10 m, driven mostly by beam size and divergence. In fact, with a 0.5 mrad divergence, we expect the beam to be 5 mm wide at 10 m.

In DUNE, we aim to reach a similar precision. This will require a number of design and installation considerations: having encoders of similar high accuracy, carrying out surveys in various reference frames, and a capability to do location checks with a precision of about 5 mm at 20 m from the beam origin. Therefore we aim to have a system that can locate the beam end point in few positions and attached to different references, at least one per drift volume and laser beam. The independent laser beam location system is described in Section 6.3.3.

Coverage estimations and top FC penetration A crucial aspect of the design of the full array is the position of the periscope and the cold mirror with respect to the FC, since its profiles can induce significant shadows and limit the beam's coverage. In order to address this aspect and

motivate the design choices, we carried out a set of shadowing calculation studies.

Given that the FC profiles are 4.6 cm wide with only a small 1.4 cm gap between them, the shadows produced if the laser source is located outside the FC would be substantial. We estimate that the maximum angle at which beams can go through is about 45°. Given the limitations of the region above the FC (shown in Figure 6.7, left), especially the geometry of the ground plane, it is likely that the mirror cannot be placed much higher up than 40 cm away from the FC. With those assumptions, we have carried out a rough estimation of the fraction of voxels that would be crossed by any unblocked track. For simplicity, we are considering only a single vertical plane, so the coverage is actually overestimated since it does not consider the effect of the FC I-beams, transverse to the FC profiles. Figure 6.7 (right) shows an example of those calculations. Assuming 10 cm voxels and no track directed at the APA, the coverage is at most 30 %. Assuming 30 cm voxels and allowing all tracks directed at the APA, the maximum coverage would be 58 %.

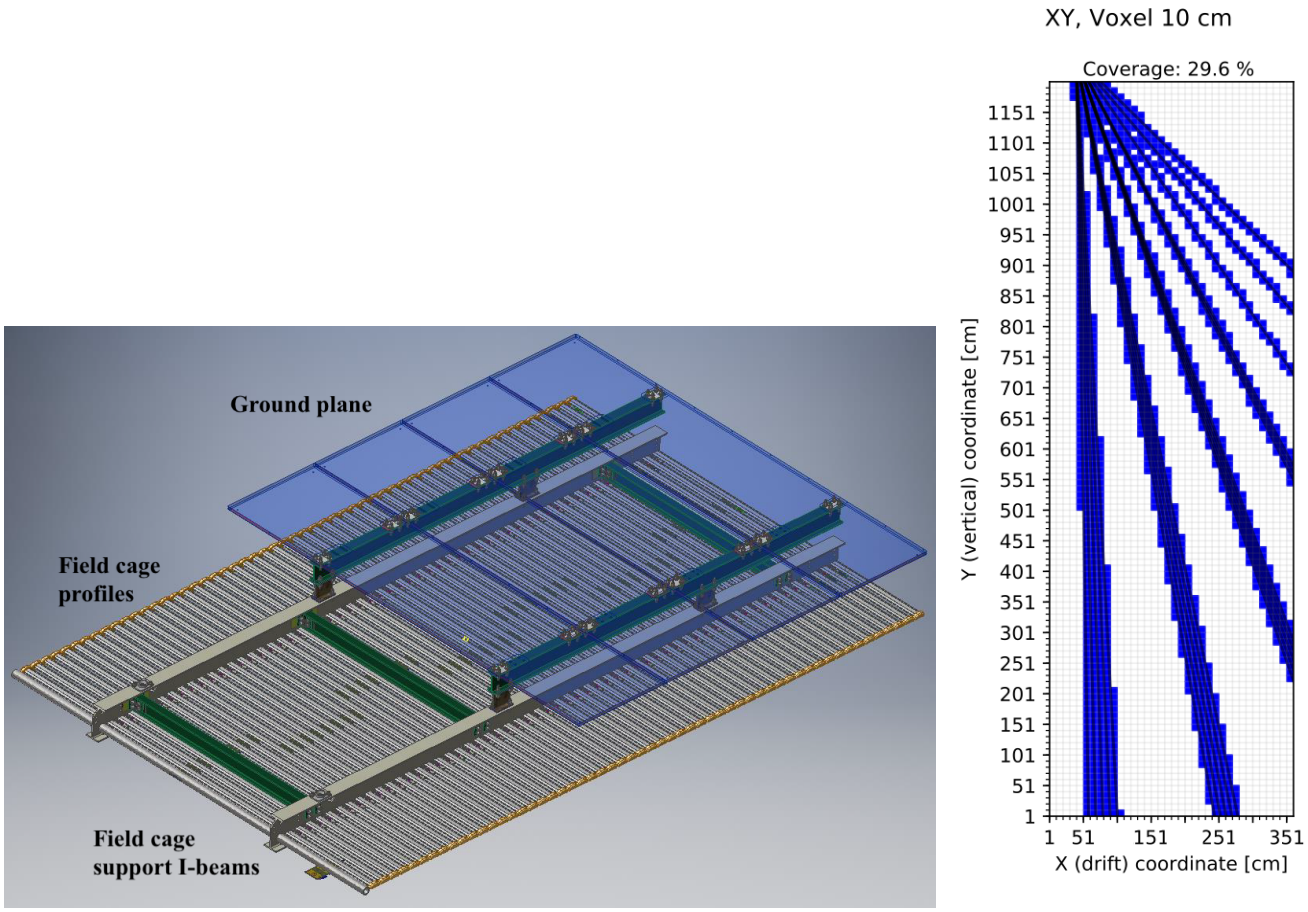

Figure 6.7: View of the top field cage (left) and laser 2D voxel coverage estimation for one drift volume (right).

Penetration of the FC would eliminate most of these shadows and allow for a practically unimpeded coverage. Depending on the depth of the periscope within the TPC, some partial shadowing from the field cage support I-beam would still remain. Figure 6.8 shows a possible way to accomplish this for the top-of-TPC ports [112]. A CAD model of the SBND laser calibration system periscope was used as reference design for DUNE. The SBND periscope, when rotating over its axis, requires

a 12 cm diameter circular region free of impediments. In order to take into account a tolerance for the estimated 0.3 % shrinkage of the FC at cryogenic temperatures, we chose an opening of three profiles, equivalent to 18 cm. Still, in order to minimize any risk associated with the presence of material close to the FC, ongoing design studies will evaluate the feasibility of implementing vertically retractable periscopes, with a travel range sufficient for them to clear the top of the FC.

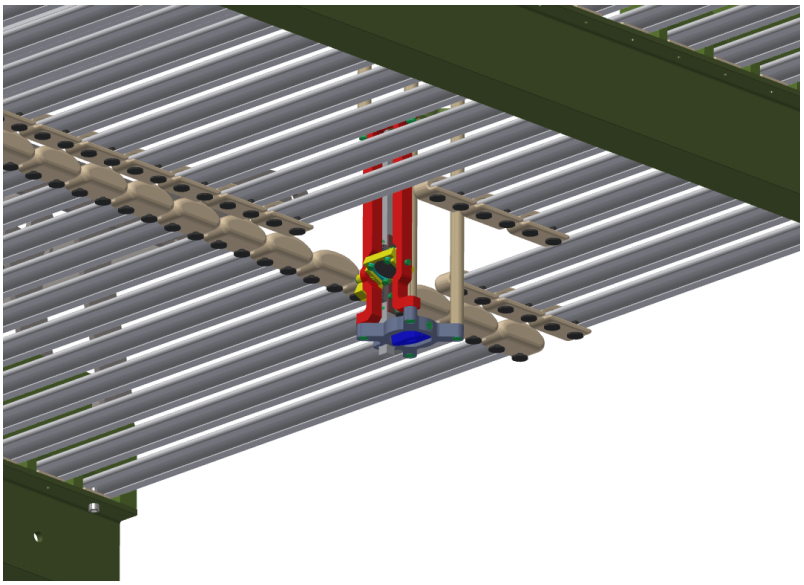

Figure 6.8: CAD drawing of one way the periscope could penetrate the FC [112].

Simulations of the effect of FC penetrations on the E field were carried out [113], and are illustrated in Figure 6.9. These have shown that the effect of a 12 cm × 12 cm opening (equivalent to two profiles), located at 40 cm (along the x direction) from the APA, is small and tolerable, with a maximum 10 kV · cm^{-1} E field caused by the opening and periscope. These simulations need to be redone with a larger opening of 18 cm × 18 cm (i.e., three profiles). Still, if we were to choose, conservatively, to discard from the physics data analysis the volume within the TPC determined by the periscope lateral size, a vertical penetration of 10 cm, and the full drift length (12 cm × 10 cm × 360 cm = 43 l for each of the 12 periscopes), it would represent only a very small fraction of 5×10^{-6} of the full detector volume.

Full array scope considerations As mentioned earlier (Section 6.3.2.2), the system should allow for crossing laser beam tracks wherever possible. In order to collect them in the full SP module volume, that would require using all the available 20 calibration ports. Since it is possible to use an iterative method to obtain displacement maps in regions where no crossing tracks are available, to minimize the overall cost of the system, the baseline design will use only the 12 central ports, providing crossing tracks in essentially 50 % of the detector volume. In addition, for the six most central ports, close to the central APA, the distance between them is small enough that we can consider having the same laser box serve two feedthroughs to reduce the costs associated with the laser and its optics. In that case, the total number of lasers needed would be nine.

Usage of the end-wall ports, which are not on top of the TPC, is therefore not part of the baseline design, and is considered only as an alternative in Section 6.7.1. A coverage calculation for possible

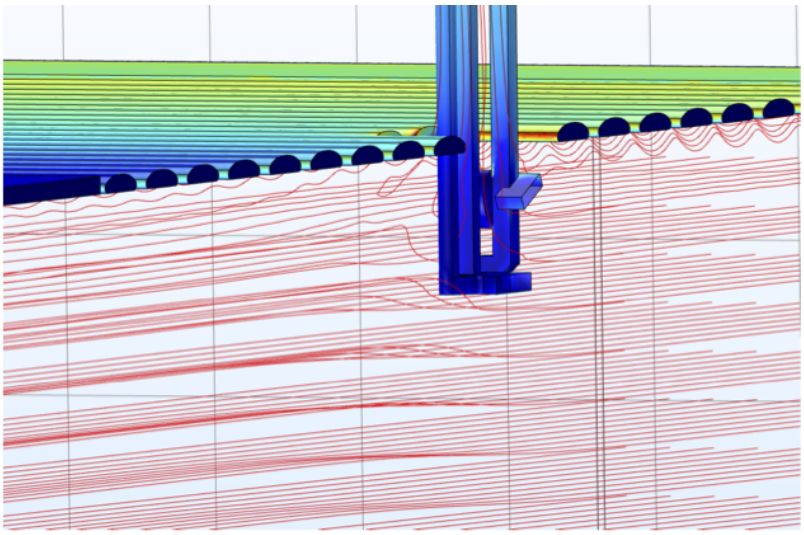

Figure 6.9: Simulation of the effect on the E field of a laser periscope penetration of the FC. In this case, an opening of only two profiles was considered.

end-wall periscopes, taking into account the shadowing of both the FC profiles and the support beams, gives a maximum of 56 % coverage for 30 cm voxels (allowing all tracks directed at the APA). In this case the laser beams would enter the FC laterally and FC penetration would be harder to consider, so an alternative mechanical design aimed at improving the coverage, is considered in Section 6.7.1.

A scan of the full detector using $10\times10\times10\,\mathrm{cm}^3$ volume elements would require a number of tracks approximately 8×10^5 and can take about three days. Shorter runs could be done to investigate specific regions. The sampling granularity, and therefore the amount of data taken, depends on DAQ requirements. In fact, even to be able to record the desired 8×10^5 tracks, a dedicated data reduction algorithm must be devised, so that only a drift window of about 100 µs of data is recorded, and the position of that window depends on the beam position and direction and which wires are being read out. More details on this are given in Section 6.4.1.

6.3.2.3.1 Measurement Program

This section describes the methods used to measure parameter maps and their expected precision, given the design outlined above.

E field and drift velocity measurement The method for E field measurement is based on the measurement of apparent position displacements of the straight laser tracks. The laser produces straight tracks with a known starting position and direction. If, when reconstructed under the assumption of uniform and homogeneous drift velocity, any deviations from that are observed, they are attributed to E field distortions.

The first step in the analysis [102] is to obtain a field of position displacements by comparing

the known and reconstructed tracks. If two crossing tracks are used, the displacement vector is simply given by the vector connecting the point where the reconstructed tracks cross and the point where the known tracks cross. However, since those displacements can vary both in direction and magnitude, there will be ambiguity in that determination if only one track is used in a given spatial region. An iterative procedure was developed by the MicroBooNE collaboration [110, 102] to obtain a displacement map from a set of several non-crossing tracks from opposite directions. Following this, a set of drift velocity field lines, which are the same as E field lines, can be obtained from the displacement map, assuming that all charge deposits along a field line will be collected in the same position. Using the relationship between E field and drift velocity [97, 103], we can then also obtain the magnitude of the E field.

Since the observed position distortion in one location depends on E field distortions in many locations along the drift path, this method of analysis clearly requires the acquisition of data from many different tracks crossing each detector drift volume at many different angles.

As already indicated in the previous section (section 6.3.2.3), the pointing precision will be on average 2 mm (at average distances of 10 m), and the TPC precision is 2 mm in x and 5 mm in y, z. Conservatively taking those in quadrature, we get $\sigma_x = 3\,\text{mm}$ and $\sigma_{yz} = 5.4\,\text{mm}$. If we would use only one track per direction, in regions of size $l = 300\,\text{mm}$, we would therefore be sensitive to drift velocity field distortions of σ/l, i.e., 1 % in x and 1.8 % in y, z.

In order to estimate the E field precision, we must distinguish between the x and y, z coordinates. To first order, distortion in y, z do not affect the magnitude of the field, and so the relative distortions on E field are equal to the relative distortions of the velocity. Along x, we must consider the relation between the magnitudes of the drift velocity and E field. Using the formula from [97, 103] we can see that, at 500 V/cm, a 1 % change in E field leads to a corresponding change of 0.375 % in drift velocity. We therefore reach the values of 2.7 % (= 1./0.375) in x and 1.8 % in y, z for a conservative estimate of E field precision using a single track per direction.

This is a conservative estimate because it does not take into account the fact that the centroid of the beam should be known better than its full width, and because it is based on the assumption of a single track per direction. As observed in MicroBooNE [102], using several tracks improves the precision, and in most of the volume an accuracy of 1 % was reached so the amount of statistics needed to reach 1 % will be an important question to address in the development plan.

On one side, this gives us an ultimate limit to the E field precision achievable with the laser system, but on the other side, since these TPC precision considerations apply to physics events also, it tells us that an E field precision much better than 1 % should not have an effect on the physics.

Charge-based measurements Electron drift-lifetime [114, 115] is the parameter that governs the dependence of the amount of collected charge on the drift time. A possible measurement of electron drift-lifetime would therefore require a very good control over the charge profile of the ionization laser tracks. This was achieved in a small scale experiment that measured lifetime with laser beams [101], but is harder with longer distances. The charge produced by the laser tracks along its path depends on distance because the light intensity is reduced due to beam divergence and scattering, as well as non-linear effects such as the self-focusing, or Kerr effect. For this reason,

the first steps in any laser-based charge measurement are a fine-tuning of the laser intensity in order to reduce self-focusing to a minimum, and "charge profile calibration scan" which consists of acquiring tracks parallel to the APA. In order to get good statistical precision, several tracks could be acquired, in the same or different direction, but always parallel to the APA in order to factorize out any effect from electron drift-lifetime. This set of data provides a calibrated laser beam charge profile that can then be used to analyse and normalize the measured charge profile from tracks that do have an angle with respect to the APA and therefore span different drift times.

As for electron-ion recombination, since the dE/dx for laser beams is much smaller than for charged particles, the effect should also be much smaller. However, that small effect has been observed [111], so a similar method than described above could be used to evaluate any dependence of the electron-ion recombination factor on the angle ϕ between the track and the electric field, that is predicted in some models [116]. This would entail taking data with tracks as parallel as possible to the E field, in order to enhance the angular dependence term on the recombination expression (that goes with $1/sin\phi$), and to compensate for the smaller dE/dx for laser beams.

6.3.3 Laser Calibration: Beam Location System

Because the precision of the E field measurement relies heavily on a precise knowledge of the laser beam tracks, an independent measurement of their direction for some specific positions is required. The laser beam location system (LBLS) addresses this requirement. While the direction of the laser beam will be very well known based on the reading from the encoders on the laser beam steering mechanism, residual uncertainty or unpredictable shift in the pointing direction will remain. Keeping in mind the long length of the ionization track of more than 15 m, even a small offset in the pointing direction can lead to vastly different ionization track locations, especially close to the end of the track. Such inaccuracies will directly affect our ability to precisely calibrate any variations in the E field.

6.3.3.1 Design

The LBLS is designed to provide precise and accurate knowledge of the laser track coordinates. Two complementary systems are planned, one based on PIN diodes and another based on mirrors.

PIN diode system for laser beam location The design for the system using PIN diodes is based on the existing system that was built for the miniCAPTAIN experiment [108].

The LBLS consists of groups of 9 PIN diodes, operating in passive, photovoltaic mode. These are GaP diodes with a sensitivity range extending down to 200 nm wavelength; thus, detecting 266 nm light is straightforward. PIN diodes are placed at the bottom of the cryostat and receive direct laser light[3] passing through the gaps between the FC profiles to minimize interference with the

[3]This is a difference with respect to the miniCAPTAIN system, which does not observe direct light, but detects fluorescence in the FR-4.

FC. Drawings of one such group of PIN diodes are shown in Figure 6.10. With the group of 9 photodiodes, we can detect not only the beam but also crudely characterize its profile, giving a more precise location of the central beam pulse axis.

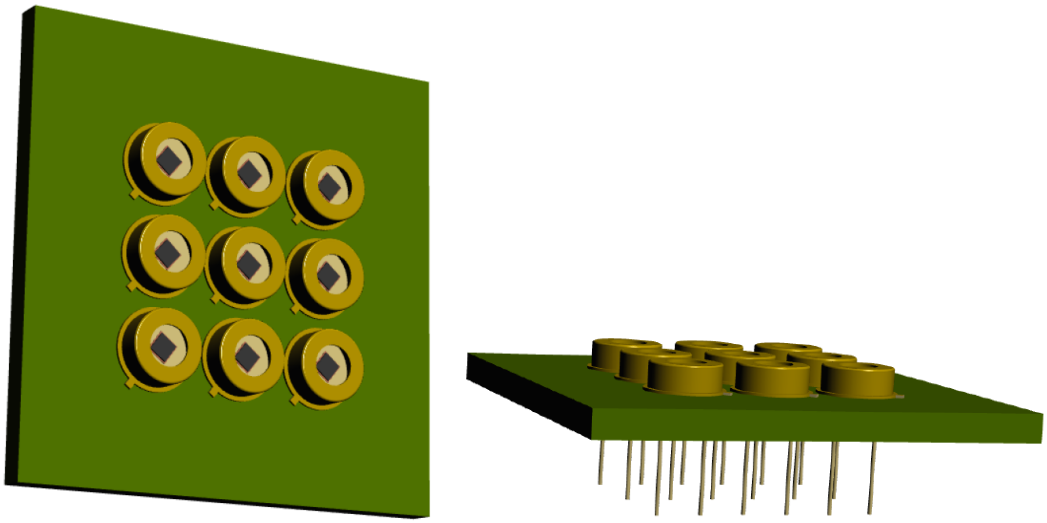

Figure 6.10: (Left) LBLS cluster mounted on the opposite wall from the laser periscope to detect and accurately determine the end point of the laser beam. (Right) Profile of the LBLS group mounted on the PCB. GaP diodes come with pins that use pair of twisted wires to transport the signal.

There will be two LBLS pads per laser, with each pad visible by two different lasers, to maximize precision and ensure sufficient redundancy in the system. There will be a total of 16 locations (4 per volume) for a total of 32 pads. Pads will be placed on the central line of each of the four volumes, in the middle between each pair of adjacent lasers, located under the FC. The locations of the pads will be carefully surveyed after installation and prior to closing of the cryostat. The laser should always send the first pulse in the direction of the LBLS before proceeding into a calibration sequence. In this way, the absolute location of the initial laser track will be determined with high accuracy. The location of the other laser tracks will also be determined with high accuracy with respect to the initial track thanks to the high precision of the rotary encoders.

Mirror-based beam location system: In addition to the PIN diode system, we will also have clusters of small mirrors that allow measuring the beam end position via its reflections.

Figure 6.11 shows a conceptual sketch with a cluster of 6 mirrors located close to each other, but with different angles. When the beam hits one of the mirrors, it will be reflected back into the TPC, and the reflection angle unambiguously identifies which mirror was actually hit. With small mirrors, 5 mm in diameter, the required positioning precision would be met if these mirrors are placed at distances of more than 10 m. The preferred location is, therefore, at the bottom FC. Because the cluster can be small (a few cm), it can fit inside the FC profiles. For each drift volume segment seen by two lasers, we plan to install at least two clusters, for redundancy, so the total number of clusters would be 32.

The simplest solution would be to use polished aluminum as the reflecting surface, so that the cluster could be a single block. Tests of the actual reflectivity of the (oxidized) surface will be part

of the development plan. An alternative would be small dielectric mirrors.

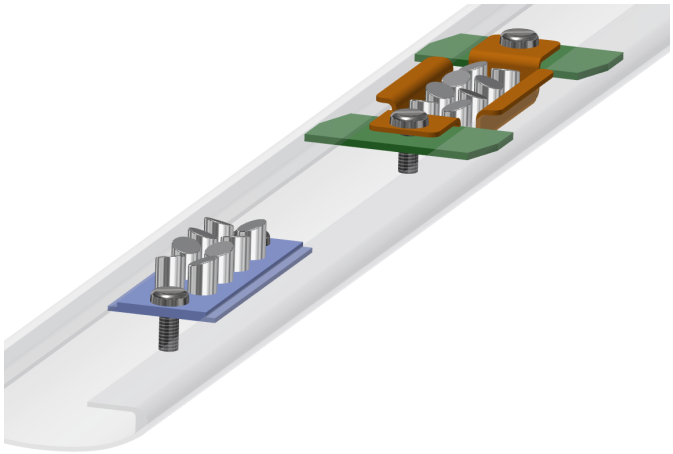

Figure 6.11: View of the mirror cluster for the beam location system inserted in the FC profiles [112].

6.3.3.2 Development plan

Further optimization of the PIN diode assembly to reduce electronic noise and cross-talk is required. Also, the size and shape of the cluster that would best collect the light coming through the field cage gaps needs to be optimized. Another important aspect is durability of the system that will require extensive running in the cryogenic conditions with a large number of cool-downs to validate GaP for extended use in DUNE. Finally, alternatives to GaP diodes such as SiPMs are under consideration. While SiPMs require power, their sensitivity to single photons makes them a desirable candidate for low light signals and more accurate beam direction reconstruction.

As for the mirror-based system, the capability of the TPC to identify the reflected beam will depend on how diffuse the reflectivity on the aluminum surfaces will be. A full test must be carried out at ProtoDUNE-SP, including alternative options such as using mirrors. Small dielectric mirrors for 266 nm with 6.35 mm diameter are commercially available.

6.3.4 Laser Calibration: Photoelectron System

Well localized electron sources represent excellent calibration tools for the study of electron transport in the LArTPC. A photoelectron laser system can provide such sources at predetermined locations on the cathode, leading to precise measurements of total drift time and integrated spatial distortions when the charge is not collected in the expected wires. These are achieved by simply measuring the time difference between the laser pulse trigger time and the time when the electron cloud reaches the APA. Such measurement will result in an improved spatial characterization of the E field, and consequent reduction of detector instrumentation systematic errors.

Being an operationally simpler system compared to the ionization laser system, the photoelectron laser can be used as a “wake-up” system to quickly diagnose if the detector is alive, and to

provide indications of detector regions that may require a fine-grained check with the ionization system. This is especially important due to the low cosmic ray environment in the detector underground. The photoelectric laser system will utilize the ionization laser for target illumination, thus eliminating the additional cost associated with the laser purchase.

6.3.4.1 Design

In order to produce localized clouds of electrons using a photoelectric effect, small metal discs will be placed on the cathode plane assembly and used as targets. Photoelectric laser systems have been successfully used at T2K [117] and in the Brookhaven National Laboratory (BNL) LAr test-stand [118] to generate well-localized electron clouds for E field calibration.

The baseline material choice for the metal targets is aluminum, while silver is being considered as an alternative. At 266 nm (Nd:YAG quadrupled wavelength) the single photon energy of 4.66 eV is sufficient to generate photoelectrons from aluminum and silver. However, aluminum and silver are prone to oxidization. In the case of aluminum, a thick layer of aluminum oxide forms the surface, but this does not increase the work function of the material. Table 6.3 lists the relevant features of metals under consideration.

The main factor driving the electron yield from the photoelectric targets is the quantum efficiency of the material. Although electrons will be released from the metal whenever photons hit the metal surface, most of the ejected electrons carry forward momentum and therefore are never released from the metal. Only a small fraction of released electrons back-scatters or knocks another electron out of the surface. The quantum efficiency for various metals is typically between 10^{-5} and 10^{-6}, thus quite low. All material candidates will be studied in the lab to verify the electron yield, and tested in ProtoDUNE-2 in order to verify the quantum efficiency for different materials.

Table 6.3: Work function and other features of candidate metal targets for laser photoelectron system.

Target Material	Work function (eV)	λ_{max} (nm)	λ_{laser} required (nm)	Oxidizing in air	Type of oxidization
Aluminum	4.06	305	266	Yes	Surface layer
Silver	4.26-4.73 (lattice dependent)	291	266	Yes	Surface layer

Disc targets will be fabricated with two different diameters: 5 mm and 10 mm to provide a test of the vertex reconstruction precision. In addition to circular targets, metal strips 0.5 × 10 cm are being considered to calibrate the rate of transverse diffusion in LAr. However, their impact on the cathode field will be carefully studied before being incorporated into target list, to prevent any disruptions to the cathode electric field.

The targets will be fastened to field shaping strips located on the rim around the resistive panel of the cathode plane assembly. Figure 6.12 illustrates locating the photoelectric targets on the rim around the resistive panel. The distance between the dots will be 10 cm with 5 targets at each corner, while the strips will be fastened at the center of each long side of the resistive plane. The

total number of disc targets per resistive panel is 20 and the total number of strips per resistive panel is 2 as illustrated in Figure 6.13. Given that there are 600 resistive panels per SP module, there will be a total of 12,000 disc targets and 1200 strip targets per module. The photoelectric dots and strips layout will be further refined based on the calibration requirements and performance simulation results. It will be essential to conduct a survey of the photocathode disc locations on the cathode after installation and prior to detector closing. In this way, the absolute spatial calibration of the E field will be achieved.

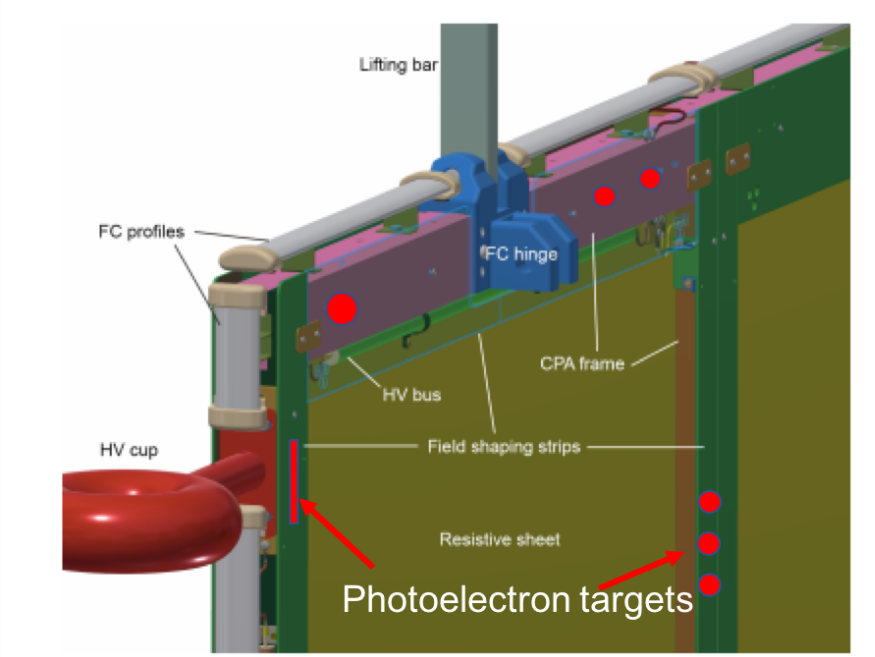

Figure 6.12: The best place to place the photo targets without being intrusive for the E field, is the surface of the field shaping strips around the rim of the resistive panel. Circular targets will be implemented, while the strip targets are still under consideration.

A few thousand electrons are required per spill from each dot to produce the signal above the noise level on the wire and this number will be achieved with high intensity lasers (pulses of the order of 100 mJ). The laser beams used to illuminate the targets will be injected into the cryostat via cryogenic optical fibers guided into mounting points in the APA, where they are coupled with defocusing elements that will illuminate 10 m diameter surface on the CPA with a single fiber. Fibers will be fastened along the central line of the APA in the space between the top and bottom APA, on the top of the upper APA and on the bottom of the lower APA. With the aid of the defocusing elements, the entire single phase module can be illuminated with a total of 72 fibers, corresponding to just 6 fibers along the central line along with 6 fibers on top and bottom for a total of 18 fibers per each of the four drift volumes. Figure 6.14 shows the conceptual view of the CPA illumination.

While the current plan aims for illumination of the entire CPA, the Kapton material that composes the resistive panels undergoes photoelectric effect, albeit with three orders of magnitude lower quantum efficiency at cryogenic temperatures when compared to phototargets at 266 nm. While the noise produced is expected to be tolerable, in case the noise is higher than anticipated, the solution is to illuminate only the areas where phototargets are placed reducing the resistive panel

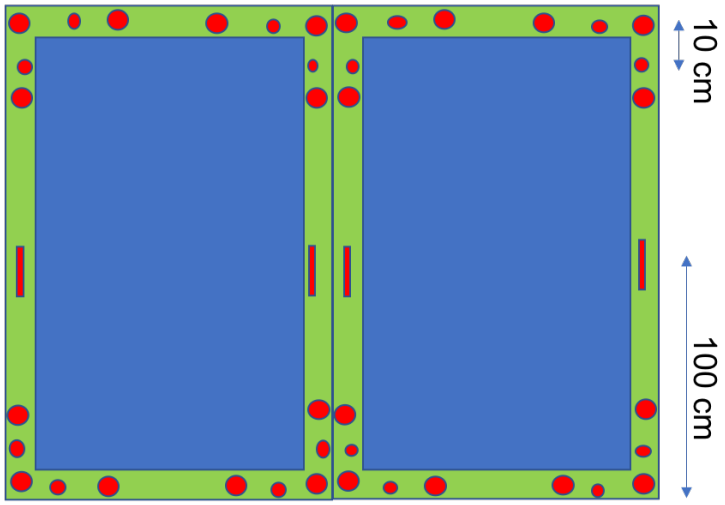

Figure 6.13: There are a total of 5 circular targets in each corner, for a total of 20 circular targets: 12 large and 8 small diameter targets total. In addition, 2 strips at the center along the long sides of the resistive panels may be added if not disruptive to the high voltage on the cathode plane.

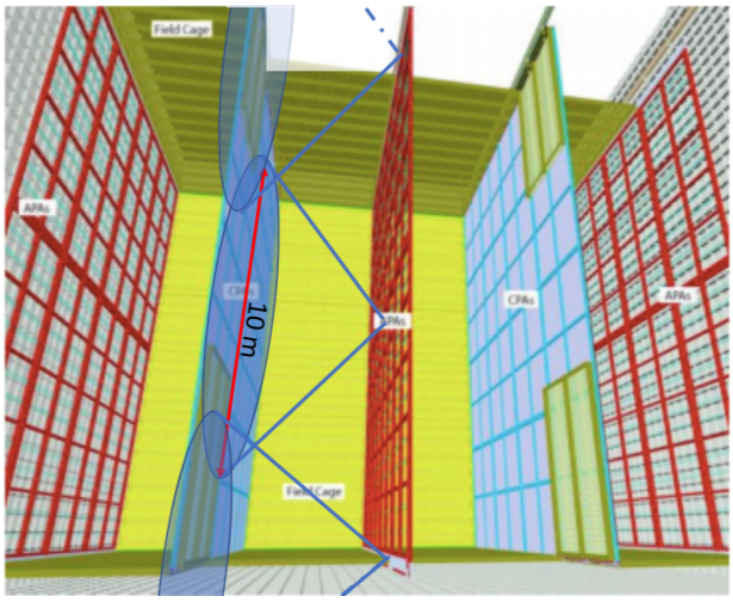

Figure 6.14: Conceptual view of the CPA illumination with fibers placed on the top and bottom of the APA for better coverage and overlap.

exposure. In this case, instead of defocusing elements, bare fibers will be utilized. The bare fiber opening angle is 10° and 1.3 m diameter exposure. Assuming parallel running of lasers, photoelectron targets in 3 out of 4 volumes can be illuminated at once, assuming that laser firing can be coordinated and calibrated with sufficient precision and that volumes 2 and 3 share lasers. Lasers typically operate at 10 Hz frequency. If 10000 pulses per laser are assumed, about 15 minutes of running is needed per laser for a single calibration run as the photoelectron clouds from different dots are very well localized. With the help of commercial multiplexers per each volume, 1 hour per volume will be sufficient for a single calibration campaign. If the DAQ or lasers themselves prevent parallel running, the entire calibration campaign will take between 15 minutes or up to 1-5 hours. The calibration run duration will depend on the final calibration scheme.

The photoelectron system will use the same lasers used for argon ionization. Stability of the laser pulses will be monitored with a power meter. Dielectric mirrors reflective to 266 nm light will guide the laser light to injection points, but a fraction of the light will be transmitted instead of reflected to the power meter behind the mirror. The laser will also send a forced trigger signal to the DAQ based on the photodiode that will be triggered on the fraction of the light passing through the dielectric mirror.

6.3.4.2 Development plan

The photoelectron system will require the following tasks to complete the design that can be done in ProtoDUNE-2 or in the lab:

- test the mounting of the targets on the CPA;
- use different target materials to compare their performance;
- verify the potential of targets to generate several 1000 electron clouds and their ability to diagnose electric field distortions and vertex reconstruction;
- allocate ports to insert laser fibers used for illumination;
- validate interface with ionization laser in order to inject UV photons into fibers;
- validate efficiency of laser light injection in the optical fiber;
- validate light attenuation in fibers;
- validate design interface with APA and optimized locations of fibers between top and bottom APAs;
- validate diffuser design and light losses in the diffuser as well as its ability to illuminate large areas of CPAs;
- validate bare fiber CPA illumination; and
- survey of the dots position to the required level of precision.

6.3.4.3 Measurement Program

Photoelectron systems have been used in other experiments to diagnose electronics issues by using the known time period between the triggered laser signal and read out times, and to perform rapid checks of the readout of the TPC itself.

A photoelectron laser is an effective diagnostic and calibration tool, that can quickly and accurately sample the electron drift velocity in the entire detector. In addition, it can be used to identify electric field distortions due to space charge effects. Exact knowledge of the timing and position of the generated electron clouds is useful for vertex calibration. In addition to electronics issues, discrepancies between the measured and expected drift time can point to either distortions in the position of the detector elements or to a different drift velocity magnitude.

Another planned measurement is the comparison between the expected and measured y, z position of the collected charge, that can point to transverse distortions of the E field.

6.3.5 Pulsed Neutron Source System

The SNB signal includes low-energy electrons, gammas and neutrons, which capture on argon. Each signal channel will have specific detector threshold effects, energy scale, and energy resolution. As noted in Volume II, DUNE Physics, Chapter 7, the sensitivity to SNB physics depends on the uncertainties of relevant detector response parameters, and so a calibration method to constrain those uncertainties is needed. Local detector conditions may change with time due to a variety of causes that include electronics noise, misalignments, fluid flow, LAr purity, electron lifetime and E field. While these are intended to be characterized from other systems via inputs to the detector model, "standard candles" provide a method to assess if our detector model is incomplete or insufficient. An ideal standard candle matches one of the relevant signal processes and will provide spatial and/or temporal information. The pulsed neutron source (PNS) system, as described below, will provide a standard candle neutron capture signal (6.1 MeV multi-gamma cascade) across the entire DUNE volume that is directly relevant to the supernova physics signal characterization. The PNS is also capable of providing a spatially fine-grained measurement of electron lifetime.

Liquid argon is near transparent to neutrons with an energy near or at 57 keV due to an anti-resonance in the cross-section caused by the destructive interference between two high level states of the ^{40}Ar nucleus (see Figure 6.15). The cross-section at the anti-resonance "dip" is about 10 keV wide, and at the bottom the cross section of 1.6×10^{-4} b implies an elastic scattering length of over 2000 m. Natural argon has three major isotopes: ^{36}Ar (0.3336 %), ^{38}Ar (0.0834 %), and ^{40}Ar (99.6035 %) each with a slightly different anti-resonance. The average elastic scattering length of the 57 keV neutrons in natural liquid argon is about 30 m.

The neutrons at the anti-resonance energy could be injected into liquid argon in the TPC, provided no materials (e.g., hydrocarbons) block the path. Those that do scatter lose energy, leave the anti-resonance, quickly slow down and are captured. Each capture releases exactly the binding energy difference between ^{40}Ar and ^{41}Ar, about 6.1 MeV in the form of γ rays. As will be described

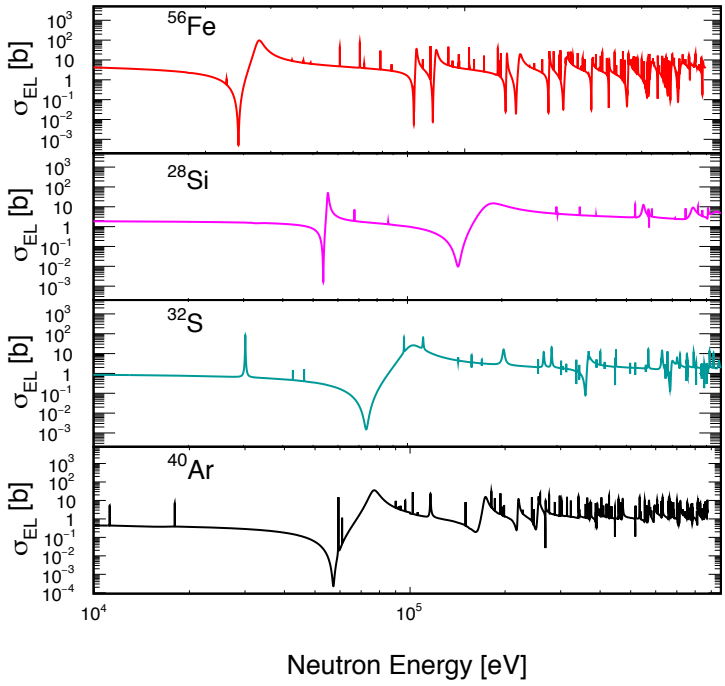

Figure 6.15: Illustration of interference anti-resonance dips in the cross section of ^{56}Fe, ^{28}Si, ^{32}S, and ^{40}Ar. Elastic scattering cross-section data is obtained from ENDF VIII.0 [**?**].

below, by using a *DD* Generator (where *DD* stands for "deuterium-deuterium"), a triggered pulse of neutrons can be generated outside the TPC, then injected via a dedicated opening in the insulation into the liquid argon, where it spreads through the 58 m volume of the detector to produce 6.1 MeV energy depositions.

One important property of the neutron capture reaction ^{40}Ar(n,γ)^{41}Ar is that the deexcitation of ^{41}Ar nucleus produces a cascade of prompt γs. Because of the detector threshold effect, the multiplicity and the total energy of the γs within the cascades could be effectively decreased to below the expected values of the neutron capture process. As a consequence, the neutron capture identification and the assessment of neutron tagging efficiency in liquid argon strongly depends on a precise model of the full γ energy spectrum from thermal neutron capture reaction. The neutron capture cross-section and the γ spectrum have been measured and characterized by the Argon Capture Experiment at DANCE (ACED), where DANCE is the Detector for Advanced Neutron Capture Experiments. Recently, the ACED collaboration performed a neutron capture experiment using DANCE at the Los Alamos Neutron Science Center (LANSCE). The result of neutron capture cross-section was published [119] and will be used to prepare a database for the neutron capture studies. The data analysis of the energy spectrum of correlated γ cascades from neutron captures is underway and will be published soon. The γ energy spectrum and the branching ratios in the ENDF library will be updated with the ACED result.

Figure 6.16 shows an example of the energy spectra of individual γ clusters measured by ACED [119]. The most common γ cascade emitted from ^{41}Ar decay has 167 keV, 1.2 MeV and 4.7 MeV γs. The peak energy of these γs can be clearly seen in the background subtracted data in Ref. [119]. In liquid argon detectors, the γs are detected through calorimetric measurement. Assuming the γ

cascade from a neutron capture is fully contained in the active volume, it is possible to detect the individual γs from the neutron capture. The correlation of the measured γ is a strong indication of neutron capture events. Low energy γ reconstruction algorithms are being investigated to identify the neutron capture events that could be used for detector response calibration.

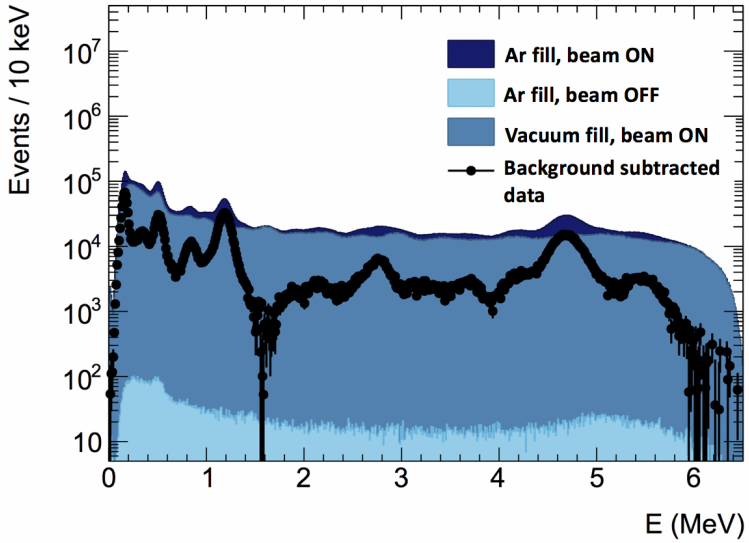

Figure 6.16: Energy spectra of individual γ clusters measured by ACED. Only events detected in the 0.02 eV to 0.04 eV neutron energy window are selected.

6.3.5.1 Design

The basic design concept of sources like the pulsed neutron source are based on successful boron neutron capture therapy [120]. The design of the PNS system used for energy calibration is shown in Figure 6.17. The system will consist of four main components: a DD generator, an energy moderator reducing the energy of the DD neutrons down to the desired level, shielding materials, and a neutron monitor to confirm neutron flux and safe operation.

DD generator source: DD generators are commercial devices that can be readily obtained from several vendors at a cost of about \$125k each, which includes all control electronics. The pulse width is adjustable and can be delivered from about 10 µs to 1000 µs (which affects the total neutron output).

Moderator: A feasible moderator has been designed using a layered moderator (Fe or Si)-filter (S)-absorber (Li) configuration. The 2.5 MeV neutrons from the DD generator are slowed to less than 1 MeV by the energy moderator. Natural iron and silicon are found to be efficient moderators for this purpose. Then an energy filter made of sulfur powder is used to further select the neutrons with the desired anti-resonance energy. The neutron anti-resonance energy in ^{32}S is 73 keV, right above the 57 keV anti-resonance energy in ^{40}Ar. The neutrons at this energy lose about 3.0 keV per elastic scattering length. After a few elastic scattering interactions, most of the 73 keV neutrons selected by the sulfur filter will fall into the 57 keV anti-resonance energy region in LAr. These materials require no cooling or special handling. Finally, a thermal absorbing volume of lithium is

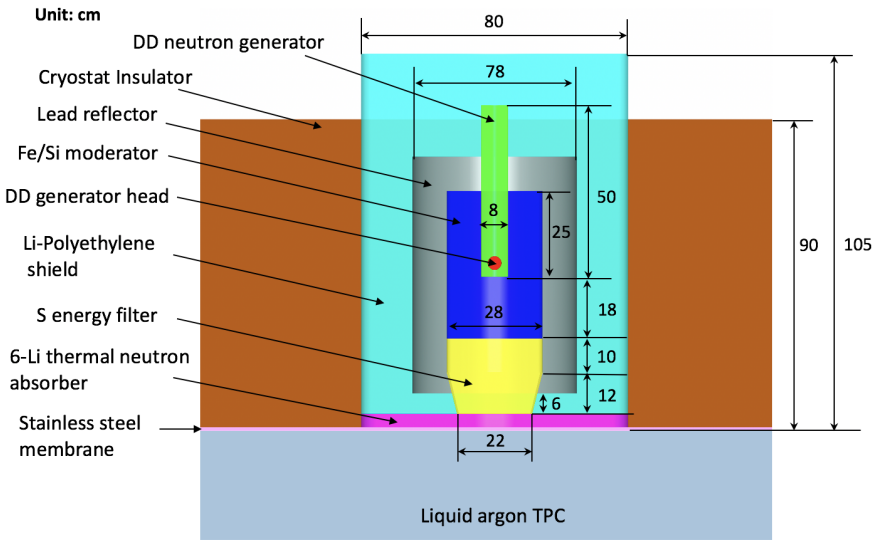

Figure 6.17: Conceptual design of the pulsed neutron source. The whole device is placed outside the TPC volume on top of the cryostat.

placed at the entry to the argon pool in order to capture any neutrons that may have fallen below the 57 keV threshold. A reflecting volume is added around the DD generator and the neutron moderator to increase downward neutron flux. Figure 6.18 shows the energy spectrum of the neutrons moderated and injected into the TPC.

Shielding: The source will be encased in a shielding volume. The goal of the shield is to block both scattered neutrons and gammas that are produced in the source. Lithium-polyethylene (7.5 %) is chosen to be the material for the neutron shield because it is rich in hydrogen and lithium atoms which yield a high neutron absorption cross section. Lithium-polyethylene is also light weight, commercially available, and relatively inexpensive. The energy spectrum entering the shield has multiple peaks between 0.5 MeV and 1.5 MeV, and one major spike at 2.2 MeV. The shield can effectively block the lower energy peaks but can only degrade the intensity of the 2.2 MeV because 2.2 MeV gammas are a characteristic signature for neutron captures on hydrogen. A safe thickness of the lithium-polyethylene shield must be found, one that can degrade the dose of 2.2 MeV gammas to safe levels. The dose of radiation from 2.2 MeV gammas was calculated assuming a person standing 1 m away. Simulation indicates that a shield with 12 cm thick lithium-polyethylene satisfies basic safety requirements[4].

Neutron Monitor: The system will need a monitoring system to confirm that the source is operating as expected. A neutron monitoring detector consisting of an Eljen EJ-420 coupled to an ADIT L51B16S 2-inch photomultiplier tube (PMT) will be placed just outside of the moderating material surrounding the DD generator and will be read out with a CAEN waveform digitizer with neutron/γ pulse-shape discriminating firmware. The monitoring detector will provide relative flux information to the calibration users and will ensure that the intensity of the source is constant, thereby allowing a comparison of data taking at different times. A small collimator will be placed in front of the neutron detector, and inside the shielding material of the DD source. The collimator

[4]These calculations will be redone assuming a 30 cm personnel safety distance and shielding thickness reestimated to meet DUNE safety requirements.

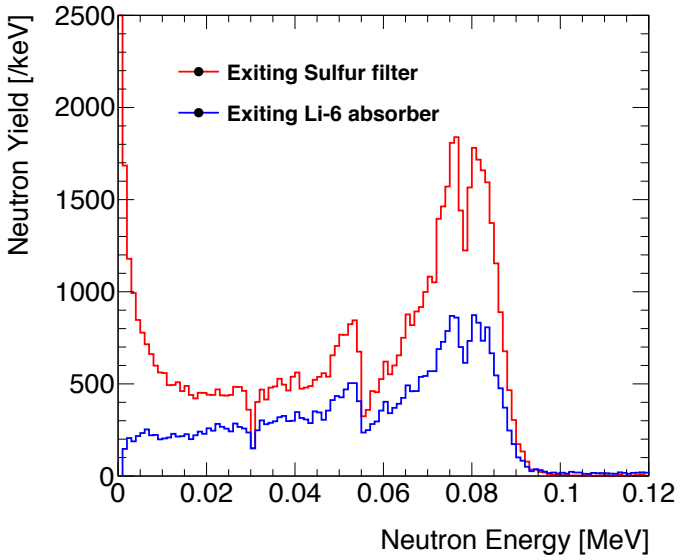

Figure 6.18: Energy of moderated neutrons produced by the pulsed neutron source. The total number of initial DD generator neutrons is 1×10^6.

dimensions and material specifications (likely a combination of iron, lead, and polyethylene) will be optimized from Monte Carlo simulations.

Based on the general concept described above, Figure 6.19 shows a conceptual layout of the neutron injection system. It is referred to as the "large format moderator" design. The neutron source is about 0.8 m wide and 1 m high. It would sit above the cryostat insulator. Beneath the neutron source, a cylindrical insulator volume with a diameter of more than 50 cm has to be removed to allow the neutrons enter the cryostat. Such an interface is provided by the human access ports near the endwalls of the detector. The top flange of the human access port is sealed, and the neutron source sits on top, providing heat insulation. The neutron source weighs about 1.6 t and will be supported by the I-beams. This design allows a permanent deployment of the neutron source. GEANT4 simulation has shown that 0.13 % of the neutrons generated by the DD generator are expected to be captured inside the TPC. It is also possible to place the neutron source inside the human access ports which would allow a factor of 6 increase of the neutron flux but will require a modification of the interface flange. This is currently being investigated.

Simulation studies were done placing the PNS system on top of a cryostat with the same size as the DUNE 10 kt TPC. Initial simulation results indicate that one PNS could cover 1/3 of the TPC volume, so three identical neutron sources on top of the cryostat would illuminate the whole TPC volume of the DUNE FD. However, this would require opening three additional neutron injection ports which are not included in the current cryostat design[5]. The baseline configuration of the PNS system consists of two large format neutron sources permanently located at the corner human access ports at the opposite ends on top of the cryostat.

[5]Ideally, opening three identical neutron injection ports for each 10 kt TPC would make full use of the neutron source. While this is not possible for the first FD module as the cryostat design is frozen, it informs the importance of these ports for subsequent FD modules.

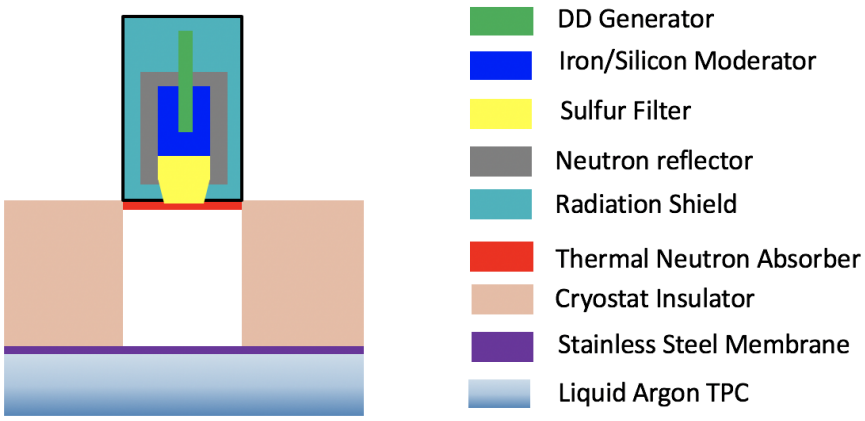

Figure 6.19: Large format neutron source deployed above/inside the human access holes.

Figure 6.20 shows the position distribution of the neutron captures under baseline configuration. The distribution shows that the baseline deployment can cover a large fraction of the TPC volume, but, as evident from the figure, not many neutrons reach the central region of the TPC. Neutrons with long scattering lengths can reach the center of the TPC but, much longer operation time maybe needed to achieve the required statistics. Assuming a minimum number of 100 neutron captures per m^3 in order to carry out a localized energy calibration, and the typical DD generator pulse intensity of 10^5 neutrons/pulse, the number of pulses needed to calibrate the high rate regions is of the order of 1000, and at least 10 times that for the low rate regions. But given the 0.5 Hz DAQ limitation, this would mean calibration runs will increase from 40 minutes to about 7 hours to cover the low rate regions. More details on this are given in Section 6.4.1. If the neutron capture events at the center of the TPC are not sufficient, the detector response calibration would depend on simulations and extrapolation using results from the regions with high neutron coverage. To increase the low coverage at the center of the TPC, an alternative deployment strategy is proposed using a small format neutron source design described in Section 6.7.2.

The system is expected to have a long lifetime of operation, as the PNS system sits on top of the cryostat, with no opening to the LAr, so it is possible to replace the system in case of failure with only crane support.

6.3.5.2 Measurement Program

The 6.1 MeV γ cascade will provide a uniform signal for neutron capture, part of the supernova signal. The source may also be used to determine the relative efficiency across the detector for neutron capture, and provide measurements of energy resolution and energy scale spatially and temporally. Simulation studies are currently underway.

The first goal of the simulation is to provide the expected distribution of signals, with a normalization given by the pulse width of PNS operation, and neutrons energy and angular correlated distribution, depending on the source filter and shield design. It is envisaged that the calibration

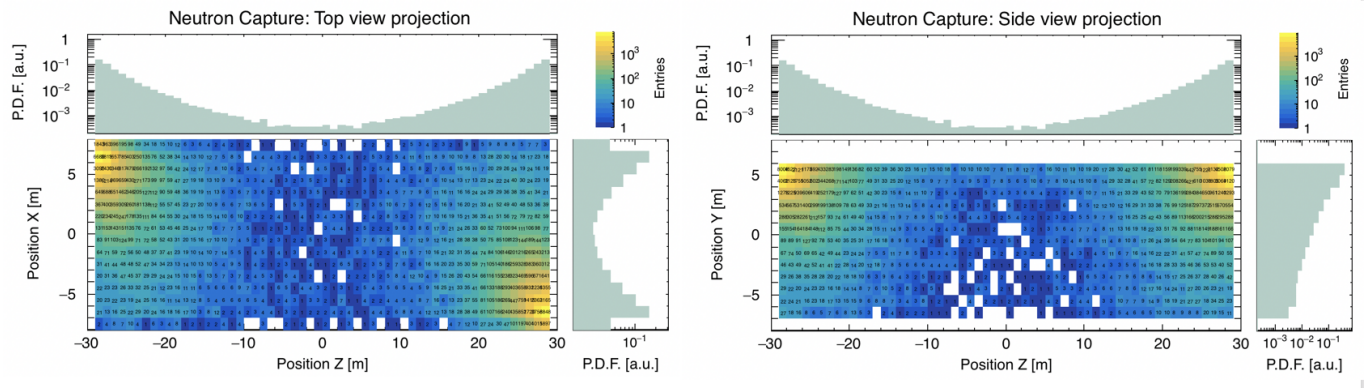

Figure 6.20: Neutron capture positions inside a DUNE-sized TPC, assuming baseline configuration with two large format neutron sources located at the corner human access ports at the opposite corners on top of the cryostat. L=60 m (along Z axis, horizontally parallel to the beam direction), W=14.5 m (along X axis, horizontally perpendicular to the beam direction), H=10 m (along Y axis, vertically perpendicular to the beam direction). 1.8×10^7 DD generator neutrons with 2.5 MeV energy were simulated in each moderator and propagated inside the TPC. Top (left) and side (right) views of neutron capture positions are shown.

can be done in two modes. First, a short PNS pulse can provide isolated neutron captures closer to the entrance path; and then a longer pulse, for which the same region is saturated, but captures happen in the full volume.

By using an external trigger coupled to the PNS operation and running the usual trigger algorithms in parallel, the calibration will provide the efficiency of the trigger and DAQ systems as a function of total fluxes. Changing the pulse width can result in higher or lower detector activity. The source will be used for SNB calibration to test the capabilities of triggering for low energy signals, but also to identify them in different pile-up conditions. The transmission of the global timing from the external PNS trigger to the DAQ provides a strong constraint on the initial timing for the TPC as the neutron capture times are of the order of 0.15 ms, much lower than typical drift time for the TPC. The PD system, with resolution of 100 ns, can discriminate between different neutron captures. The calibration will measure the efficiency of the PD system response for low energy events, depending on the distance due to Rayleigh scattering in LAr. We will then study the usage of the PD system time information for improving the position reconstruction of TPC signals. In the absence of the PD system system, the global timing from the PNS translates to an uncertainty of around 10 cm.

Individual event positions can be translated into response maps of both the photon detectors and the LArTPC to standard candles of 6.1 MeV electromagnetic depositions. When the cascades can be more precisely reconstructed, individual γs within the cascades can be identified, and this provides a lower energy "standard candle" close to the solar electron-neutrino threshold. Comparing the collected charge for equal energy signals at different distances from the TPC gives a measurement of the electron lifetime, a key detector response parameter. High PNS flux runs can generate momentary local space charge effects, in the upper regions of the detector, that will need to be characterized; low flux runs should be taken before to ensure expected space charge distributions. The global simulation will be tested in the (smaller scale) ProtoDUNE detectors.

The neutron mean free path will be larger than the ProtoDUNE size, and so external events and interactions with materials of the PD system, APA, and CPA systems will be more prominent. These effects must be simulated.

Note that captures of external background neutrons, entering the active volume is a main background for low energy physics; a comparison of simulations of PNS events and external neutron backgrounds will be interesting, as will a comparison of simulated supernova and solar neutrino signals. For the high energy beam events, the number and energy distributions of neutrons depend on the type of neutrino interaction and are significantly different for neutrinos and anti-neutrinos. Measuring the number and distance of neutron captures around the main hadronic cascades can thus help in identifying which extra proton scattering signals to associate to the hadronic cascades. This can also help make a statistical correction to the energy reconstruction of the neutrino and anti-neutrino events.

6.3.6 Validation of Calibration Systems

All calibration designs presented in the previous section require full system validation before being deployed in the DUNE FD. Here, we describe the validation of a complete baseline design and some of the alternative designs described in the Appendix, Section 6.7.

Although laser calibration systems are being operated in other LArTPC experiments (e.g., MicroBooNE, future SBND runs), they have stringent requirements in terms of mechanical and optical precision , long-term reliability, laser track length, performance of the LBLS, DAQ interface, and effect on E field, especially due to the FC penetration. All of these lead to corresponding goals for a test installation and operation in ProtoDUNE-SP that could be done in the post-LS2 run. As Figure 6.21 shows, ProtoDUNE-SP has ports of the same size as the DUNE FD that could be used for these tests. If a pair of ports can be used, then one could even have crossing tracks within a single drift volume. If one of the ports external to the TPC can be used, then we would test the double-rotary alternative system described in Section 6.7.1 and aimed at improving the coverage from the end-wall locations.

The goal for validation would be to test all aspects of the system design, installation, alignment, operation, interfaces with DAQ, and analysis, among others. ProtoDUNE-SP, because it is located at the surface, could measure the E field map with cosmic rays to compare with the one from the laser system to improve the analysis methods or identify weak aspects in the design. An important design parameter is the length of a laser track. Our design assumes that 20 m is possible. MicroBooNE has demonstrated only up to 10 m, but the track could be longer, depending on laser intensity. Measurements are limited by the size of the detector, but one way to gain information on longer tracks is to make a scan with low laser intensities, so that the end of the track is visible, and register how the maximum obtained track length scales with intensity. An extrapolation to the DUNE FD laser intensity would tell us the maximum length possible. Such a measurement could also be done at MicroBooNE or SBND.

An important aspect of the development plan, to be carried out at ProtoDUNE-SP-2, is the characterization of the charge created by the laser beam ionization as a function of distance travelled in

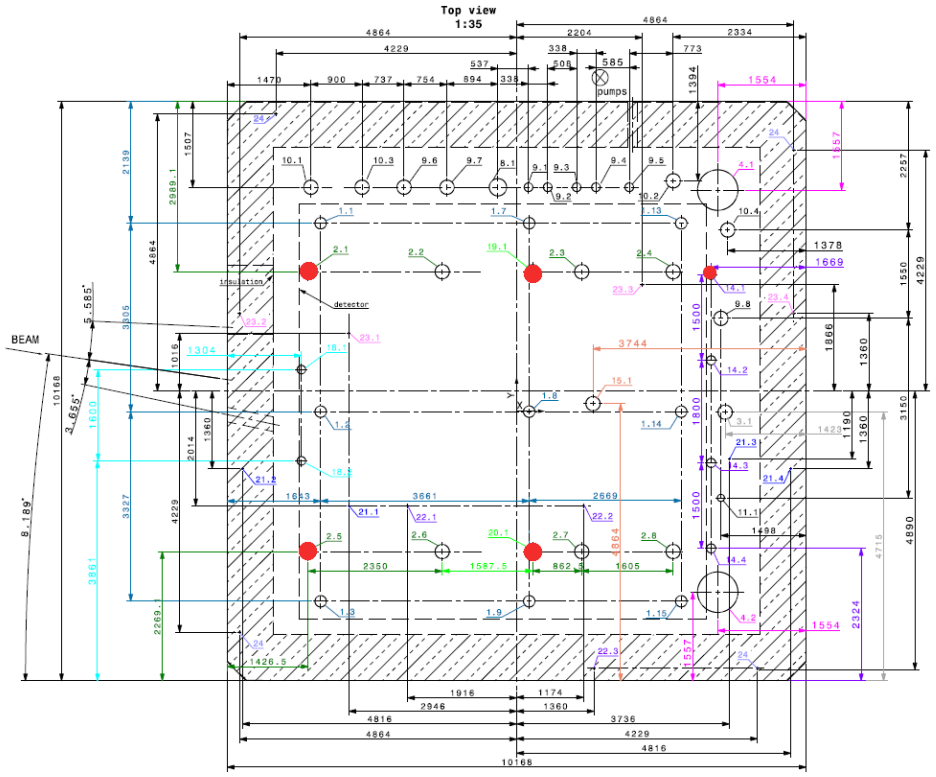

Figure 6.21: Top view of the ProtoDUNE-SP cryostat showing various penetrations. Ports marked in red are free and could be used to test the calibration systems. The four largest ports have the same diameter (250 mm) as the calibration ports of DUNE FD, and are located over the TPC. The largest ports at the right side corners of the cryostat are the human access ports.

the LAr and the laser beam intensity. This dependence is thought to be affected by self-focusing effects due to the high light intensity, but it can be studied by measuring the collected charge distribution from a series of tracks close, and parallel, to the APAs in order to break any correlations with the electron lifetime. This measured charge function could then be used with tracks in different directions to obtain a measurement of electron lifetime, which would significantly increase the capabilities of the laser system.

The pulsed neutron source is a new idea never used in other experiments, so a ProtoDUNE-SP-2 test is essential. The corner human access ports similar to the ones in the DUNE FD could be used for this test.

In addition to dedicated hardware validation runs at ProtoDUNE-SP-2, other LAr experiments provide ample opportunities to develop and validate calibration tools and techniques, especially those relevant to the hardware being deployed. For example, the MicroBooNE experiment is currently leading the development of analysis methods using laser data to extract an E field map. Energy calibration techniques and related software tools are also being developed at various experiments (MicroBooNE, ICARUS, LArIAT, ProtoDUNE) that involve estimating and propagating uncertainties like E field distortions, recombination, and other effects into physics signals. Other calibration related developments include DAQ and calibration database design, all of which are being improved at SBN and ProtoDUNE.

6.4 Interfaces with other Consortia

Interfaces between calibration and other consortia have been identified and appropriate documents have been developed. The documents are currently maintained in the CERN Engineering and Equipment Data Management Service (EDMS) database, with a TDR snapshot kept in the DUNE document database (DocDB). DUNE document database (DocDB). A brief summary is provided in this section. Table 6.4 lists the interfaces and corresponding DocDB document numbers. The main systems calibration has interfaces with are HV, PD system, and DAQ, and the important issues that must be considered are listed below.

HV Evaluate the effect of the calibration hardware on the E field due to laser system periscopes and FC penetration. Evaluate the effect of the incident laser beam on the CPA material (Kapton); Integrate the hardware of the photoelectron laser system (targets) and the LBLS (diodes) within the HV system components. Ensure that the radioactive source deployment is in a safe field region and cannot do mechanical harm to the FC.

PDS Evaluate long term effects of laser light, even if just diffuse or reflected, on the scintillating components (tetra-phenyl butadiene (TPB) plates) of the PD system; establish a laser run plan to avoid direct hits; evaluate the effect of laser light on alternative PD system ideas, such as having reflectors on the cathode plane assemblies; validate light response model and triggering for low energy signals.

DAQ Evaluate DAQ constraints on the total volume of calibration data that can be acquired;

develop strategies to maximize the efficiency of data taking with data reduction methods; study how to implement a way for the calibration systems to receive trigger signals from DAQ to maximize supernova live time. More details on this are presented in Section 6.4.1.

Integrating and installing calibration devices will interfere with other devices, requiring coordination with the appropriate consortia as needed. Similarly, calibration will have significant interfaces at several levels with cryostat and facilities in coordinating resources for assembly, integration, installation, and commissioning (e.g., networking, cabling, safety). Rack space distribution and interaction between calibration and systems from other consortia will be managed by technical coordination in consultation with those consortia.

Table 6.4: Calibration Consortium Interface Links.

Interfacing System	Description	Reference
HV	effect of calibration hardware (laser and radioactive source) on E field and field cage; laser light effect on CPA materials, field cage penetrations; attachment of positioning targets to HV supports	DocDB 7066 [33]
PD system	effect of laser light on PD system, reflectors on the CPAs (if any); validation of light response and triggering for low energy signals	DocDB 7051 [90]
DAQ	DAQ constraint on total volume of the calibration data; receiving triggers from DAQ	DocDB 7069 [121]
CISC	multi-functional CISC/calibration ports; space sharing around ports; fluid flow validation; slow controls and monitoring for calibration quantities	DocDB 7072 [122]
TPC Electronics	Noise, electronics calibration	DocDB 7054 [75]
APA	APA alignment studies using laser and impact on calibrations	DocDB 7048 [17]
Physics	tools to study impact of calibrations on physics	DocDB 6865 [123]
Software and Computing	Calibration database design and maintenance	DocDB 6868 [124]
TC Facility	Significant interfaces at multiple levels	DocDB 6829 [125]
TC Installation	Significant interfaces at multiple levels	DocDB 6847 [126]

6.4.1 Calibration Data Volume Estimates

The calibration systems must interface with the DUNE DAQ system, discussed in detail in Chapter 7. Trigger decisions for physics events are made hierarchically: trigger primitives are generated from TPC and PD system "hits", and these trigger primitives are then used to create trigger candidates which are collections of trigger primitives satisfying selection criteria such as exceeding a threshold number of adjacent collection wire hits, or total collection wire charge recorded, etc. These trigger candidates are passed on to a module level trigger (MLT) which then makes decisions about whether a given trigger candidate is accepted as a detector-wide trigger. If so, the MLT sends trigger commands to the data flow orchestrator (DFO) which in turn passes them to an available event builder (EB) that then requests data from the front-end (FE) readout of the DAQ (servers that host Front-End Link eXchange (FELIX) cards). The management of trigger decisions—whether they are generated by candidates from the TPC, PD system, calibrations, or other systems—is done in the MLT.

The trigger commands are in the form of absolute time stamps that are used to extract snapshots of the data stored in the FE readout buffers. For physics triggers, all TPC information for a snapshot of time (roughly twice the drift time, or 5.4 ms) are read out, without any additional zero suppression or localization. For calibration events, this approach would create an unmanageable amount of data and, in any case, is unnecessary because calibration events create interactions or tracks at known positions or times, or both.

To reduce data volume from calibrations, therefore, calibration systems that can be triggered externally are desirable. Like the distribution of trigger commands to the FE readout buffers, the external trigger for a calibration system will take the form of an absolute time stamp. The time stamp is generated by the MLT, thus ensuring that (for example) a calibration event does not occur during a candidate supernova burst. The distribution of these time stamps will be done through the DAQ's timing and synchronization system. Thus triggerable calibration systems (like the laser or PNS) will have to be synchronized to the rest of the DAQ system and be capable of accepting time stamps. There will be differences in the details of how different calibration systems are handled, as discussed later in this section.

Table 6.5 shows the estimated data volume needs for various calibration systems assuming each system is run twice per year. For the ionization laser system, as noted earlier, a scan of the full detector can take about three days, resulting in a total of about six days or a week per year per 10 kt module. For the PNS system, as noted later in this section, a single run can take about seven hours; doing that twice, or even four times, per year will result in a total of about one day per year per 10 kt module. It is expected that once the detector launches into stable operations, the need for full calibration campaign runs will reduce to one nominal run per year. We also expect some shorter runs may be needed in smaller, targeted regions of the detector, or for detector diagnostic issues.

Table 6.5: Estimated data volume needs per year per 10 kt for various calibration systems.

System	Data Volume (TB/year)	Assumptions
Ionization Laser System	184	800k laser pulses, $10\times10\times10\,\mathrm{cm}^3$ voxel sizes, a 100 µs zero suppression window (lossy readout), and 2 times/year
Neutron Source System	144	10^5 neutrons/pulse, 100 neutron captures/m^3, 130 observed neutron captures per pulse, 2 times/year

6.4.1.1 Laser System

The E field vector from ionization laser calibration is determined by looking at the deflection of crossing laser tracks within detector voxels. Because any given laser track illuminates many such voxels, one laser pulse can be used for several measurements; essentially, what matters is how many voxels it takes to cover three walls of a given drift volume – CPA, bottom and end-wall FC, taking into account that we divide that volume by 4 because of beam coverage.

Considering a small voxel size of $10\times10\times10\,\mathrm{cm}^3$, the total number of independent track directions is estimated to be 800,000: about half the rate of cosmic rays and thus nominally a substantial total data volume. However, with the specification voxel size of $30\times30\times30\,\mathrm{cm}^3$, that number would be 27 times smaller, so that would allow a larger number of tracks per direction. Keeping to the overall estimate of 800,000 tracks per scan, the choice of voxel granularity and track statistics per direction can be made until the commissioning period.

Fortunately, unlike every other event type in the detector, the laser track has both a reasonably well known position and time; thus the trigger command issued to the FE buffers can be much narrower than the window used for physics triggers. A 100 µs zero suppression window should be wide enough to avoid windowing problems in the induction plane wire deconvolution process. To ensure that the interesting part of each waveform is recorded, the DAQ will need to know the current position of the laser, which will be transmitted from the laser system to the MLT via the DAQ control, configuration and monitoring subsystem (CCM).

From the standpoint of data volume, therefore, the total assuming the 100 µs zero-suppression window is

$$800{,}000/\mathrm{scan}/10\,\mathrm{kt} \times 100\,\mu\mathrm{s} \times 1.5\mathrm{Bytes/sample} \times 2\,\mathrm{MHz} \times 384{,}000\ \mathrm{channels} = 92\ \mathrm{TB/scan}/10\,\mathrm{kt}. \quad (6.1)$$

If such a calibration scan were done twice a year, then the total annual data volume for the laser is 184 TB/year/10 kt and four times a year would result in 368 TB/year/10 kt

6.4.1.2 Pulsed Neutron Source

The pulsed neutron source (PNS) system creates a burst of neutrons that are captured throughout a large fraction of the total cryostat volume. For triggering and data volume, this is very convenient: the existing scheme of taking 5.4 ms of data for each trigger means all these neutrons will be collected in a single DUNE event. Thus, the data volume is simply 6.22 GB times the total number of such pulses, but these are likely to be few: a single burst can produce thousands of neutrons whose t_0 is known up to the neutron capture time of 200 µs or so.

To trigger the PNS, the MLT will provide a time stamp for the source to fire, and then send a trigger command to the FE readout buffers (via the DFO and EB) that will look like a physics trigger command. The MLT itself then tags that trigger command with the expected trigger type (in this case, PNS).

Typically, a commercial DD neutron generator produces 10^5 - 10^8 neutrons/pulse, depending on the adjustable pulse width. The current assumption for neutron yield from the DD generator is 10^5 neutrons per pulse[6]. With the current baseline deployment design in Figure 6.19, approximately 130 neutron captures per DD generator pulse should be observed inside a 10 kt module. As shown in Figure 6.20, the deployment of two large format neutron sources at the corner human access ports could approximately provide calibration for about half of the total TPC volume (30 kt). As the suggested number for localized energy calibration is 100 neutron captures per m^3, a total number of 2300 pulses would be needed to calibrate regions under high neutron coverage. Assuming two identical pulsed neutron sources operating in synchronization mode, 1150 triggers are needed for each calibration run. Therefore, the total data volume per run would be

$$1150 \text{ Triggers} \times 1.5 \text{ Bytes} \times 2\,\text{MHz} \times 5.4\,\text{ms} \times 384{,}000 \text{ channels} = 7.2 \text{ TB/run}. \quad (6.2)$$

The recommended trigger rate of the PNS system is 0.5 Hz which is limited by the bandwidth of the DAQ event builder. Assuming that the spatial distribution of the neutron capture is near-uniform for the regions that are covered by the two large format neutrons sources, the operation time per calibration run would be 40 minutes. Running the PNS calibration system twice a year would result in a total data volume of 14.4 TB per 10 kt per year. For realistic neutron capture distribution that is non-uniform, we expect to operate the PNS system for a period of 10 times longer than that under the ideal assumption (7.2 TB/run). As a consequence, the data size per calibration run would be 72 TB/run and running the PNS calibration twice a year would result in a total data size of 144 TB/year/10 kt and four times a year results in 288 TB/year/10 kt.

[6] Realistic assumption based on commercially available DD generators that produce the most neutron yield with a pulse width less than 100 µs. DD generators with higher neutron yield are being developed in laboratories; commercial devices may require further development to reach a higher level of performance.

6.5 Construction and Installation

6.5.1 Quality Control

The manufacturer and the institutions in charge of devices will conduct a series of tests to ensure the equipment can perform its intended function as part of quality control (QC). QC also includes post-fabrication tests and tests run after shipping and installation. The overall strategy for the calibration devices is to test the systems for correct and safe operation in dedicated test stands, then at ProtoDUNE-SP-2, then as appropriate near Sanford Underground Research Facility (SURF) at South Dakota School of Mines and Technology (SDSMT), and finally underground. Electronics and racks associated to each full system will be tested before transporting them underground.

- **Ionization Laser System:** The first important test is design validation in ProtoDUNE-SP-2. For assembly and operation of the laser and feedthrough interface, this will be carried out on a mock-up flange for each of the full hardware sets (periscope, feedthrough, laser, power supply, and electronics). All operational parts (UV laser, red alignment laser, trigger photodiode, attenuator, diaphragm, movement motors, and encoders) will be tested for functionality before being transported underground.
- **Photoelectron Laser System:** The most important test is to measure the light transmission of all fibers at 266 nm. A suitable transmission acceptance threshold will be established based on studies during the development phase. Studies to estimate the number of photoelectrons emitted as a function of intensity (based on distance of fiber output to the metallic tab) will also be undertaken.
- **Laser Beam Location System:** For the LBLS, the main test is checking that the PIN diodes are all functional, and with a light detection efficiency within a specified range, to ensure uniformity across all clusters. For the mirror-based system, the reflectivity of all mirrors will also be tested prior to assembly.
- **Pulsed Neutron Source System:** The first test will be safe operation of the system in a member institution radiation-safe facility. Then, the system will be validated at ProtoDUNE-SP-2. The same procedure will be carried out for any subsequent devices before the devices are transported to SURF and underground. System operation will be tested with shielding assembled to confirm safe operating conditions and sufficient neutron yields using an external dosimeter as well as with the installed neutron monitor. The entire system, once assembled, can be brought down the Ross shaft.

6.5.2 Installation, Integration and Commissioning

This section describes the installation plans for calibration systems. Most of the hardware is to be installed outside the cryostat so, space on mezzanine surrounding each calibration port is important for powering and operating the calibration systems. However, some sub-systems have internal components which will be installed following a specific installation sequence, coordinated with other consortia.

6.5.2.1 Ionization Laser System

Checking the alignment of the optical components is an essential step of the ionization laser system installation. The system includes a low power visible laser that can be used for the several mirror alignment operations, but before that use, both the UV and the visible lasers in the laser box need to be aligned. Alignment of the visible and UV (Class 4) lasers requires special safety precautions and must be carried out once for each periscope/laser system before installing further TPC components. For that reason, the laser boxes must be installed on the cryostat roof as soon at that area becomes accessible.

The periscopes are the only components of the ionization laser system that will be inside the cryostat, but they will be installed from the top of the cryostat and not from the temporary construction opening (TCO), including the alternative options. However, this installation should be done very carefully in the presence of an operator inside the cryostat, to ensure there are no collisions of the long laser periscopes with other detector components, especially FC elements and CE cable trays. The periscopes should be installed after the relevant structural elements, especially the top FC modules. Installation should proceed in sequence with the assembly of other components, with the furthest from TCO assembled first.

The relevant QC is essentially an alignment test. The LBLS can be used to align the periscopes as they are installed, so it is important that the LBLS is also installed in the same sequence as the periscopes.

A support beam structure closest to the TCO temporarily blocks the calibration ports, but it is removed after the last TPC component is installed. After that, the final calibration components can be installed, including the periscopes on the TCO end wall.

6.5.2.2 Laser Beam Location System

This system has several parts that need to be installed inside the TCO, and some must be integrated with the HV system during installation underground.

The PIN diode system uses a set of diodes that fire when the laser beam hits them. Because the laser shoots from above and the diodes must be in a low voltage region, the plan is to place the diodes below the bottom FC, facing upward, simply on a tray close to the cryostat membrane.

For the pointing measurement, the beams will pass through the FC electrodes and hit the diodes below. There will be 32 of these diode clusters to be installed. The installation will consist of positioning the cluster trays in pre-determined locations, and routing the cables to the respective feedthroughs (work is still underway to decide how to route cables and which flanges to use).

The second laser beam location system consists of a set of 32 mirror clusters: a plastic or aluminum piece holding four to six small mirrors 6 mm in diameter, each at a different angle; the ionization laser will point to these mirrors to obtain an absolute pointing reference. These clusters will be

attached to the bottom FC profiles facing into the TPC. This attachment/assembly of the mirror clusters on corresponding FC profiles will be done during FC assembly underground.

6.5.2.3 Photoelectron Laser System

A large number of photoelectric targets (about 4000) must be attached to the cathode. Experience from other experiments indicates that targets can be glued to the cathode surface, which can be done after cathode assembly but before the cathode is installed in the cryostat.

Once the cathode plane assemblies are in place, the photoelectric target locations will need a high precision survey, which is necessary for the absolute calibration of the electric field with the photoelectron laser.

The third part of the installation is quartz optical fibers on the APA, needed to illuminate the photoelectric targets with light from the Nd:YAG laser. Fiber tips must be properly fastened and oriented for effective illumination, and fiber bundle routing will bring the fiber bundles to the outside of the cryostat where Nd:YAG laser injection points will be located.

6.5.2.4 Pulsed Neutron Source System

The PNS will be installed after the human access ports are closed because the source sits above the cryostat. Installing the system should take place in two stages. In the first stage, the assembly of the system would be independent of the TPC installation. The whole system will be assembled on the ground outside the cryostat at a dedicated radiation safe area. Once assembled, the neutron source will be lifted by crane and integrated with the cryostat structure. Final QC testing for the system will be operating the source and measuring the flux with integrated monitor and dosimeter.

6.5.3 Safety

This section discusses risks to personnel safety. Detector safety and risks involving damage to detector components are discussed in Section 6.6.3.

Human safety is of critical importance during all phases of the calibration work, including R&D, laboratory testing, prototyping (including ProtoDUNE-SP deployment), and integration and commissioning at the DUNE FD site. DUNE environment, safety and health (ES&H) personnel review and approve the work planning for all phases of work as part of the initial design review, as well as before implementation. All documentation of component cleaning, assembly, testing, installation, and operation will include hazard analysis and work planning documentation and will be reviewed appropriately before production begins. In addition, in the case of planned ProtoDUNE-2 tests, the consortium will interface with CERN safety system to ensure all requirements are met.

Several areas are of particular importance to calibration are

- **Underground laboratory safety:** All personnel working underground or in other installation facilities must follow appropriate safety training and be provided with the required personnel protective equipment (PPE). Risks associated with installing and operating the calibration devices include, among others, working at heights, confined space access, falling objects during overhead operations, and electrical hazards. Appropriate safety procedures will include aerial lift and fall protection training for working at heights. For falling objects, the corresponding safety procedures, including hard hats (brim facing down) and a well restricted safety area, will be part of the safety plan. More details on PPE are provided in TDR Volume III, DUNE Far Detector Technical Coordination, Chapter 10.
- **Laser safety:** The laser system requires operating a class IV laser [127, 128]. This requires an interlock on the laser box enclosure for normal operation, with only trained and authorized personnel present in the cavern for the one-time alignment of the laser upon installation in the feedthroughs. The trained personnel will be required to wear appropriate laser protective eye wear. A standard operating procedure will be required for the laser which will be reviewed and approved by the Fermi National Accelerator Laboratory (Fermilab) laser safety officer.
- **Radiation safety for PNS:** A DD neutron generator will be used as a calibration device. The design of safety systems for this system include key control, interlock, moderator, and shielding. Lithium-polyethylene (7.5 %) is chosen to be the material for the neutron shield which is rich in hydrogen. The gammas from neutron capture on hydrogen in the shielding material could cause potential radiation hazards. The design of the radiation safety systems (custom shielding and moderator) will be designed to meet Fermilab Radiological Control Manual (FRCM) safety requirements and will be reviewed and approved by Fermilab radiological control organization. Material safety data sheets will be submitted to the DUNE ES&H to understand other safety hazards such as fire. Before beginning any operations at ProtoDUNE-SP, the entire system will be assembled in a neutron shielded room and tested to confirm no leaking of neutrons will occur. The system will also have a neutron monitor that can provide an interlock.
- **High voltage safety:** Some of the calibration devices will use high voltage. Fabrication and testing plans will show compliance with local HV safety requirements at any institution or laboratory that conducts testing or operation, and this compliance will be reviewed as part of the design process.
- **Hazardous chemicals:** Hazardous chemicals (e.g., epoxy compounds used to attach components of the system) and cleaning compounds will be documented at the consortium management level, with a material safety data sheet as well as approved handling and disposal plans in place.
- **Liquid and gaseous cryogens:** Cryogens (e.g., liquid nitrogen and LAr) will most likely be used in testing of calibration devices. Full hazard analysis plans will be in place at the consortium management level for full module or module component testing that involves cryogens. These safety plans will be reviewed appropriately by DUNE ES&H personnel before and during production.

6.6 Organization and Management

6.6.1 Consortium Organization

The calibration consortium was formed in November 2018 as a joint single and dual phase consortium, with a consortium leader and a technical leader. Figure 6.22 shows the organization of the consortium. The calibration consortium board currently comprises institutional representatives from 11 institutions as shown in Table 6.6. The consortium leader is the spokesperson for the consortium and responsible for the overall scientific program and management of the group. The technical leader of the consortium is responsible for managing the project for the group.

The consortium's initial mandate is the design and prototyping of a laser calibration system, a neutron generator, and possibly a radioactive source system, so the consortium is organized into three working groups, each dedicated to one system. Each group has a designated working group leader.

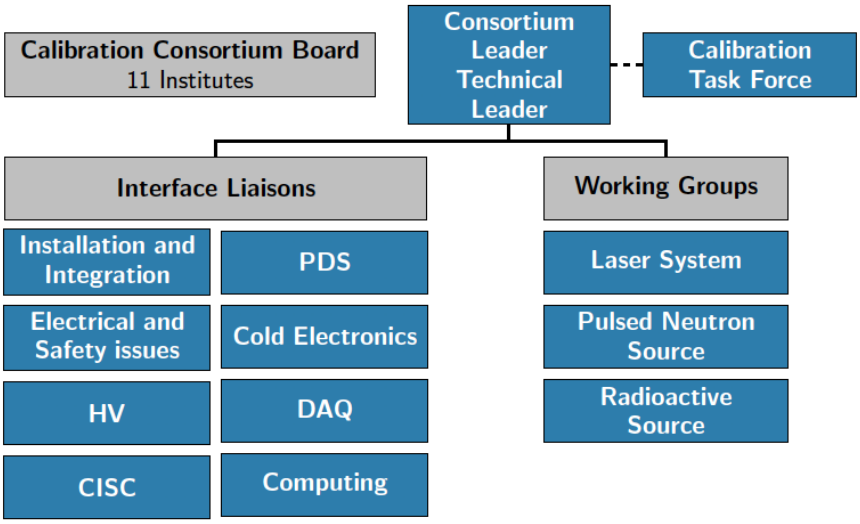

Figure 6.22: Organizational chart for the calibration consortium.

In addition, Figure 6.22 shows several liaison roles currently being established to facilitate connections with other groups and activities:

- Detector integration and installation,
- Electrical and safety issues,
- DAQ,
- Computing,
- Cryogenic instrumentation and slow controls (CISC),
- Cold electronics,
- High voltage,

Table 6.6: Current Calibration Consortium Board Institutional Members and Countries.

Member Institute	Country
LIP	Portugal
University of Bern (Bern)	Switzerland
Los Alamos National Lab (LANL)	USA
Michigan State University (MSU)	USA
Colorado State University (CSU)	USA
University of Iowa	USA
University of Hawaii (Hawaii)	USA
University of Pittsburgh (Pitt)	USA
Boston University (BU)	USA
University of California, Davis (UC Davis)	USA
South Dakota School of Mines and Technology (SDSMT)	USA

- Photon Detection System.

Currently, new institutions are added to the consortium following an expression of interest from the interested institute and upon obtaining consensus from the current consortium board members.

6.6.2 Institutional Responsibilities

Calibrations will be a joint effort for SP and DP. Design validation, testing, calibration, and performance of calibration devices will be evaluated using ProtoDUNE data.

Following the conceptual funding model for the consortium, various responsibilities have been distributed across institutions within the consortium. Table 6.7 shows the current institutional responsibilities for primary calibration subsystems. For physics and simulations studies and validation with ProtoDUNE, a number of institutions are interested.

6.6.3 Risks

Table 6.8 lists the possible risks identified by the calibration consortium along with corresponding mitigation strategies and impact on probability, cost, and schedule post-mitigation. The table shows all risks are medium or low level, mitigated with necessary steps and precautions. More discussion on each risk is provided below.

- *Risk 1:* The ProtoDUNE-SP design tests being inadequate for the FD is an important one because this requires early validation from ProtoDUNE data so we can perform R&D of alternate designs and/or improvements on a reasonable time scale. In addition, the calibration ports will be designed to be multipurpose to enable deployment of new systems if they are

Table 6.7: Institutional responsibilities in the Calibration Consortium

Subsystem	Institutional Responsibility
Ionization Laser System	Bern, LIP, LANL, Hawaii
laser beam location system	Hawaii, LIP
Photoelectron Laser System	LANL, Hawaii
Pulsed Neutron Source System	BU, CSU, UC Davis, Iowa, LIP, MSU, LANL, SDSMT
Proposed Radioactive Source System	SDSMT
Physics & Simulation	BU, CSU, Hawaii, LANL, LIP, MSU, SDSMT, UC Davis, Pittsburgh, Iowa

developed. Therefore, in general, the calibration systems mitigate risk to the experiment as the systems sit above the cryostat and/or use multipurpose ports and may be removed.

- *Risk 2:* This is a medium-level risk where the elements of the calibration system fail engineering requirements, such as laser beam divergence and precision of the mechanical system, in which case the as-built system will not meet the physics requirements. The mitigation strategy for this involves testing the same designs envisioned for the FD in dedicated lab tests and ProtoDUNE-SP-2, to identify any issues and address them. The pre-installation QC will also allow us to reject parts that do not meet requirements.
- *Risk 3:* If the ionization laser beam directly hits the elements of the PD system system for an extended time, the scintillation efficiency might be degraded. The mirror movement controller of the laser system must avoid the beam directly hitting the PD system. An automated system will block or turn off the laser beam in case of saturation at one of the PD system channels. The laser electrical system must allow the later implementation of a hardware interlock if that is found to be necessary.
- *Risk 4:* This is a low level risk, where the laser beam location system fails; this would reduce the precision of the E field measurement but will not prevent the measurement from being made. Pre-fill QC will be carried out to minimize this risk. Additionally, redundancy will be built into the system, with alternative targets, including some passive ones. A possible alternative way to obtain an absolute measurement is to use reflections off of the aluminum FC profiles, with a very slow angular scan.
- *Risk 5:* This risk relates to the laser beam misalignment. If the laser beam becomes misaligned with the mirror sequence, then that specific ionization laser module becomes unusable for calibration. To mitigate this, the ionization laser system includes a visible (red) laser specifically for the purpose of alignment. If the misalignment is not just with the warm mirrors, but also with the cold ones, cryostat cameras might be needed to check arrival of red light to the TPC.
- *Risk 6:* If the effective attenuation length of 57 keV neutrons in LAr turns out to be significantly smaller than 30 m, then PNS system will not cover the whole detector, or additional modules will be needed. This will be resolved in the next year by a measurement at the

Los Alamos National Lab (LANL); the ProtoDUNE run will also provide a full end-to-end demonstration.

- *Risk 7:* If the neutron flux from the *DD* generator of the PNS system is enough to activate the moderator and cryostat insulation, then a new source of radiological backgrounds might be created. This can be mitigated by neutron activation studies of insulation material, and ProtoDUNE testing at neutron flux intensities and durations well above the run plan, as well as simulation studies done in collaboration with the DUNE Background Task Force.
- *Risk 8:* If the neutron yield from the *DD* generator is not high enough to provide sufficient neutron captures inside the TPC, then either the neutron calibration cannot be done or a higher flux generator must be obtained, or additional sources must be used. Investigation is being done on both commercially available and custom *DD* generators. Additionally, operating the *DD* generator with wider pulse is under consideration, which would require the PD system to provide the neutron capture time t_0. Another possibility is to carry out dedicated runs at higher pulse rate and, to ensure that the DAQ can handle it, one would acquire only the data from the APAs farthest from the source. All of this will be tested in the ProtoDUNE-2 run. Placing the neutron source closer to the TPC may increase the neutron yield by a factor of 6. An alternative design (Figure 6.24) with neutron source inside the calibration feedthrough ports (centrally located on the cryostat) is being studied. This compact neutron source would be light enough to be moved across different feedthroughs and will provide additional coverage.
- *Risk Opportunity 9:* The ionization laser system assumes that the laser beams will be sufficiently narrow for a measurement up to 20 m distances. However, as the Rayleigh scattering is of the order 40 m, it is possible the laser may travel further than 20 m. This may reduce the number of lasers needed and therefore the overall cost. The maximum laser distance will be assessed in ProtoDUNE-2.

Table 6.8: Calibration risks (P=probability, C=cost, S=schedule) The risk probability, after taking into account the planned mitigation activities, is ranked as L (low $< 10\,\%$), M (medium $10\,\%$ to $25\,\%$), or H (high $> 25\,\%$). The cost and schedule impacts are ranked as L (cost increase $< 5\,\%$, schedule delay < 2 months), M ($5\,\%$ to $25\,\%$ and 2–6 months, respectively) and H ($> 20\,\%$ and > 2 months, respectively).

ID	Risk	Mitigation	P	C	S
RT-SP-CAL-01	Inadequate baseline design	Early detection allows R&D of alternative designs accommodated through multipurpose ports	L	M	M
RT-SP-CAL-02	Inadequate engineering or production quality	Dedicated small scale tests and full prototyping at ProtoDUNE; pre-installation QC	L	M	M
RT-SP-CAL-03	Laser impact on PDS	Mirror movement control to avoid direct hits; turn laser off in case of PDS saturation	L	L	L
RT-SP-CAL-04	Laser beam location system stops working	QC at installation time, redundancy in available targets, including passive, alternative methods	L	L	L
RT-SP-CAL-05	Laser beam misaligned	Additional (visible) laser for alignment purposes	M	L	L
RT-SP-CAL-06	The neutron anti-resonance is much less pronounced	Dedicated measurements at LANL and test at ProtoDUNE	L	L	L

RT-SP-CAL-07	Neutron activation of the moderator and cryostat	Neutron activation studies and simulations	L	L	L
RT-SP-CAL-08	Neutron yield not high enough	Simulations and tests at ProtoDUNE; alternative, movable design	L	M	M
RO-SP-CAL-09	Laser beam is stable at longer distances than designed	tests at ProtoDUNE	M	H	L

6.6.4 Schedule and Milestones

Table 6.9 shows the schedule and key milestones for the calibration consortium that lead to commissioning the first FD module. The demonstration of calibration systems design, operation, and performance at the ProtoDUNE-SP-II running is a key part of calibration schedule; those milestones are also listed in the table. The technology design decisions on calibration subsystems should be made by January 2020 for the laser system and by March 2020 for the neutron source system followed by technical design reviews. The production of design prototypes to be deployed at ProtoDUNE-SP-II running should be finished by February 2021 followed by assembly and deployment in ProtoDUNE-SP in March 2021. The radioactive source deployment system (RSDS)

design will follow a demonstration R&D program outlined in detail in Table 6.11 in the Appendix, with major milestones highlighted in this section. The major steps for systems approval are the design review in May 2020 and the deployment test at ProtoDUNE-SP-II in April 2022.

Production of calibration systems for the FD should start in March 2022, followed by assembly of the systems underground once the detector cavern becomes available in early 2023. Installing the laser system can begin as soon as the cryostat roof is accessible and conclude once the TPC is ready to install. If it is approved, the RSDS guide system can begin installation just beforeTPC is installed. The purge-boxes on top of the cryostat can be done later. Installing the main components of the PNS will begin once the human access ports are no longer needed for TPC installation in June 2025.

Table 6.9: Key calibration construction schedule milestones leading to commissioning the first FD module. (*) Schedule items related to the radioactive source deployment system (RSDS) are to be considered pending system approval.

Milestone	Date (Month YYYY)
Laser systems design decision (including ionization, beam location and photoelectron systems)	January 2020
Laser systems design review	February 2020
PNS design decision	March 2020
PNS design review	April 2020
RSDS design review	May 2020
Start of module 0 component production for ProtoDUNE-II	April 2020
End of module 0 component production for ProtoDUNE-II	February 2021
Start of ProtoDUNE-SP-II installation	March 2021
Start of ProtoDUNE-DP-II installation	March 2022
production readiness review dates	March 2022
South Dakota Logistics Warehouse available	April 2022
RSDS demonstration test at ProtoDUNE-SP-II (*)	April 2022
Start of Laser and PNS production	May 2022
Beneficial occupancy of cavern 1 and central utility cavern (CUC)	October 2022
End of PNS production	March 2023
End of Laser system production	July 2023
End of RSDS production (*)	August 2023
CUC counting room accessible	April 2023
Start assembly of calibration production units in the cavern	May 2023
Top of detector module #1 cryostat accessible	January 2024
Start installation and alignment of Laser boxes	May 2024
Start of detector module #1 TPC installation	August 2024
Start installation of Laser System periscopes	August 2024
Start installation of RSDS guide system (*)	August 2024
End of detector module #1 TPC installation	May 2025
Installation of RSDS purge-boxes (*)	May 2025
Installation of the PNS main components	June 2025
Top of detector module #2 accessible	January 2025
Start of detector module #2 TPC installation	August 2025
End of detector module #2 TPC installation	May 2026

6.7 Appendix

6.7.1 Laser System Alternative Designs

6.7.1.1 End-wall coverage enhancement

The eight calibration ports closer to the end-walls (four on each side) are not positioned on top of the TPC, but instead located about 40 cm away from the FC along the z (beamline) direction. If positioned on top, FC penetration would be quite complicated, having to come from the sides. Use of the periscope baseline design for the end-wall periscopes would severely limit the volume coverage, similar to the coverage limitation mentioned in Section 6.3.2.3.

We describe here an alternative design for the end-wall ports that would improve the laser beam coverage without requiring FC penetration.

The periscope is exactly the same as the baseline design but, at the top of the calibration port, is mounted on a flange that has an additional rotation degree of freedom. Figure 6.23 presents a preliminary drawing of the concept. The 250 mm diameter calibration port has on top of it the main rotary flange that, itself, has another smaller port off-centered by 40 mm with respect to the main one. On this smaller port, a secondary rotary flange is installed and it is this one that holds the laser periscope, including the optical feedthrough and the linear stage for mirror movement. When the main flange rotates, the periscope also moves along a circular (40 mm diameter) trajectory. Consequently, within the cryostat, the relative position between the beam mirror and the FC profiles changes as well, and so the shadowed regions also change, by parallax. Using different main rotary flange angles, it should be possible to locate the mirror in enough different positions in order to cover all the previously shadowed angles.

Calculations similar to the ones showed earlier show that, using only 3 different positions (separated by 90°), a coverage of 94 % should be possible for 30 cm voxels and allowing all tracks directed at the APA.

6.7.2 PNS System Alternative Designs

6.7.2.1 Small Format Moderator

An alternative method for delivering the neutrons is to use the existing calibration feedthroughs. In the current cryostat design, 20 calibration feedthroughs with a 25 cm outer diameter will be available on top of the cryostat. One can design the neutron source with an ultra-thin DD generator that fits the size of the feedthrough as shown in Figure 6.24 (right). The problem is that there will be no space in the feedthrough for the shielding materials to fit in, so additional shielding will need to be placed around the feedthrough. The weight of this compact neutron source will be

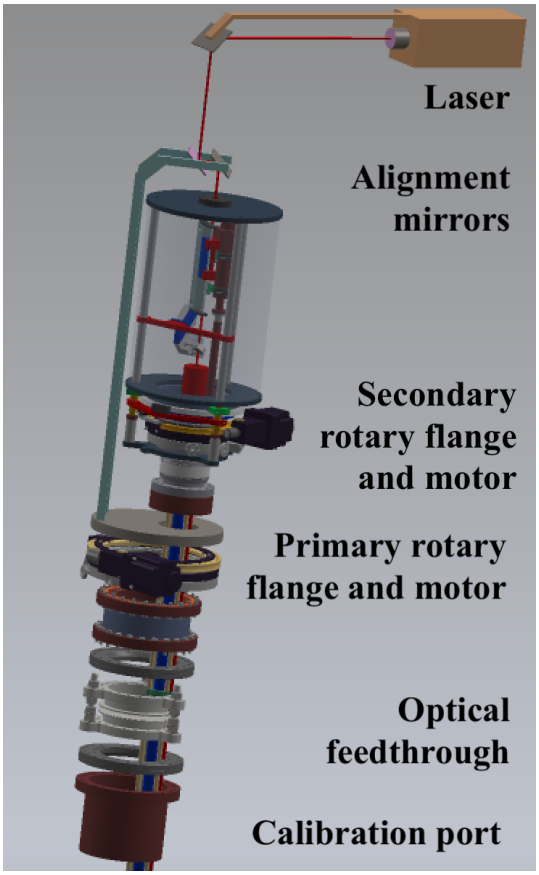

Figure 6.23: Exploded CAD drawing (preliminary) of the double rotary flange for the end-wall laser calibration ports. The calibration port is shown in brown at the bottom; the primary and secondary rotary flanges are shown in yellow, with the (black) motors next to them. The optical feedthrough is shown in the center, in blue. On top, the mirror arrangement allows the laser beam to be aligned with the optical feedthrough no matter the angle of each of the rotary flanges.

about 140 kg, so minimal special mounting is needed. In addition, the source may be moved as well, allowing further flexibility. The effective neutron flux is expected to be similar to that of the baseline deployment.

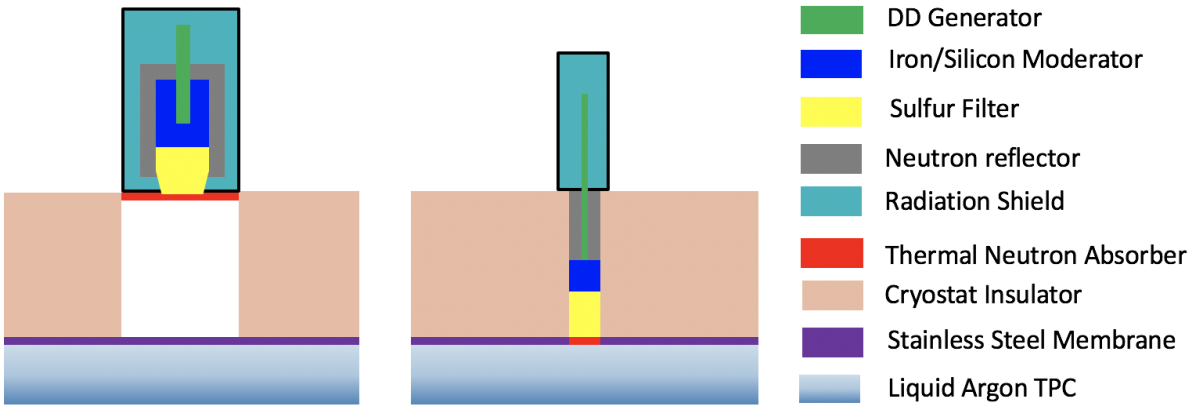

Figure 6.24: (right) Small format neutron source deployed inside the calibration feedthrough ports. (left) For comparison, large format neutron source deployed above/inside the human access ports is shown on the left.

The volume coverage at the center of the detector can be significantly increased by using a small format neutron source deployed on top at the center of the cryostat using the multi-purpose feedthroughs. Figure 6.25 shows the position distribution of the neutron captures using two large format sources at the corner human access ports and one additional small format source in the middle of the cryostat. The small format source is important to complement the coverage at the center of the TPC. The alternative small format neutron source is very compact and lightweight, so further coverage improvement is possible by moving the source to different calibration feedthroughs. The deployment of the small format source would require sharing of the feedthrough ports with other calibration systems, which is currently under investigation.

In principle, for the baseline deployment plan as shown in Figure 6.20, we can run the neutron source for a longer time to increase the coverage at the central region of the detector. However, this would result in a huge data volume. So, the best way to complement the coverage at the center of the detector is to use the alternate deployment as discussed here. This design would require a total number of 4600 pulses to calibrate the entire 10 kt module. Assuming that three neutron sources with identical neutron capture yield are operated in synchronization mode, 1500 triggers are needed for each calibration run. Therefore, the total data volume per run would be

$$1500 \text{ Triggers} \times 1.5 \text{ Bytes} \times 2\,\text{MHz} \times 5.4\,\text{ms} \times 384{,}000 \text{ channels} = 9.5 \text{ TB/run}. \quad (6.3)$$

The recommended trigger rate of the PNS system is 0.5 Hz which is limited by the bandwidth of the DAQ event builder. Assuming that the spatial distribution of the neutron capture is uniform across the whole detector volume, the operation time per calibration run would be 50 minutes. Running the PNS calibration system twice a year would result in a total data volume of 19 TB

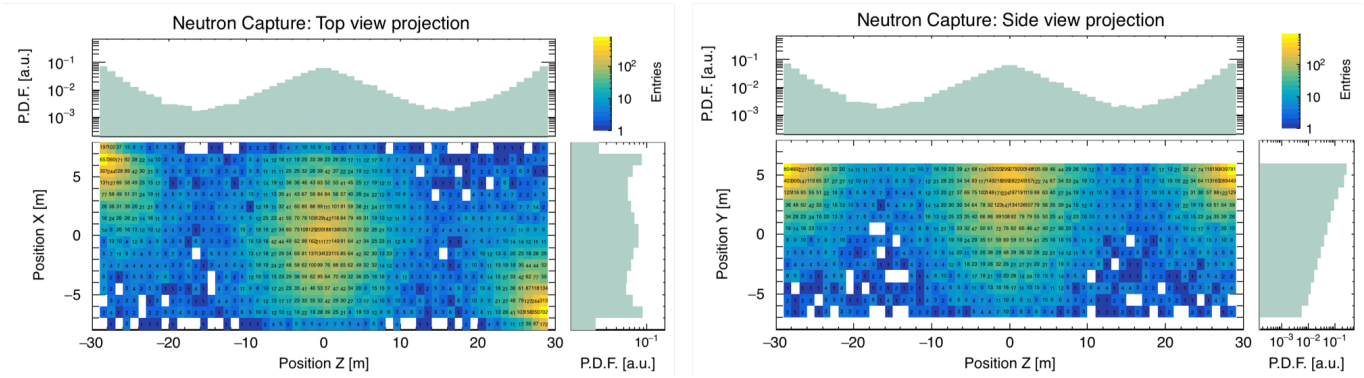

Figure 6.25: Neutron capture positions inside a DUNE-sized TPC, assuming alternative configuration with two large format neutron sources located at the corner human access ports and one small format neutron source located at the center of the cryostat, which compensates the missing volume coverage of the two large format sources at the center of the detector. L=60 m (along Z axis, horizontally parallel to the beam direction), W=14.5 m (along X axis, horizontally perpendicular to the beam direction), H=10 m (along Y axis, vertically perpendicular to the beam direction). 2.7×10^7 DD generator neutrons with 2.5 MeV energy were simulated in each moderator and propagated inside the TPC. Top (left) and side (right) views of neutron capture positions are shown.

per 10 kt per year. For realistic neutron capture distribution that is non-uniform, we expected to operate the PNS system for a period of 10 times longer than that under the ideal assumption (9.5 TB/run). As a result, the data size per calibration run would be 95 TB/run and running the PNS calibration twice a year would result in a total data size of 190 TB/year and four times a year would result in 380 TB/year.

6.7.3 Proposed Radioactive Source Calibration System

Radioactive source deployment provides an in-situ source of physics signals at a known location and with a known activity that can be chosen such that there is only one calibration event per drift time window. The primary source design probes de-excitation products (γ-rays) which are directly relevant for detection of supernova neutrinos and ^{8}B/hep solar neutrinos. The radioactive source deployment system (RSDS) is the only calibration system that could probe the detection capability for single isolated solar neutrino events and study how well radiological backgrounds can be suppressed. The trigger efficiency could be studied as a function of threshold.

Other measurements with the primary source include electro-magnetic (EM) shower characterization for long-baseline ν_e CC events, electron lifetime and electric field as a function of detector module vertical position, individual light detector response, and determination of radiative components of the Michel electron energy spectrum from muon decays. Aside from the primary nickel source that produces 9 MeV γ-rays via the ^{58}Ni(n,γ)^{59}Ni reaction, other sources could be deployed with the same multi-purpose system, for example an (α,γ) source, and ^{252}Cf and/or AmBe neutron sources that probe the impact of various radiological backgrounds, like radon (causing (α, γ) events) or radiological neutrons, or simply measure the neutron tagging efficiency, useful

for improved calorimetry of beam neutrino interactions. In contrast to the primary nickel source with 9 MeV gamma-rays, the (α,γ) source producing gamma-ray energies around 15 MeV via the ^{40}Ar(α,γ)^{44}Ca reaction could even be deployed outside of the cryostat, to probe the upper visible energy range and trigger efficiency for ^{8}B/hep solar neutrinos.

Both the RSDS and the PNS systems are needed to address the integrated response of the detector for low energy physics, especially SNB and ^{8}B/hep solar neutrinos. The RSDS primarily probes for trigger efficiency, the PNS tests mostly for uniformity. Response in argon may change rapidly as a function of photon energy due to underlying nuclear physics mechanisms. A combination of 6 MeV (direct neutron capture response), 9 MeV (from the nickel source), 15 MeV (from the (α,γ) source) is needed to map the low energy response. In terms of complementarity, radioactive sources provide a known position, known-energy single photon events that could be triggered on, while the pulsed neutron source provides a simple, potentially, non-invasive design with externally triggered multi-photon energy signature which is visible across the entire detector with a known time signature.

6.7.3.1 Design Considerations

A composite source can be used that consists of ^{252}Cf, a strong neutron emitter, and ^{58}Ni, which, via the ^{58}Ni(n,γ)^{59}Ni process, converts one of the ^{252}Cf fission neutrons, suitably moderated, to a monoenergetic 9 MeV photon [129]. The source is envisaged to be inside a cylindrical moderator with mass of about 15 kg and a diameter of 20 cm such that it can be deployed via the multipurpose instrumentation ports discussed in Section 6.3.1. The activity of the radioactive source is chosen such that no more than one 9 MeV capture γ-event occurs during a single drift period. This forms the main requirement for this system as this allows one to use the arrival time of the measured light as a t_0 and then measure the average drift time of the corresponding charge signal(s). Table 6.10 lists the full set of requirements for the radioactive source deployment system.

The sources would be deployed outside the FC within the cryostat to avoid regions with a high electric field, about 30 cm from the field cage. The γ-ray would need to travel about two attenuation lengths (including the 10 cm radius of the source body). Such high γ-energies are typically only achieved by thermal neutron capture, which invokes a neutron source surrounded by a large amount of moderator, thus driving the size of the source.

Table 6.10: Full list of Specifications for radioactive source deployment system.

Quantity/Parameter	Specification	Goal
Distance of the source from the field cage	30 cm	
Rate of 9 MeV capture γ-events inside the source (top-level requirement)	< 1 Hz	
Data volume per 10 kt	50 TB $\cdot$ year^{-1}	100 TB $\cdot$ year^{-1}
Longevity	20 years	$>$ 20 years

A gamma source based on the ^{58}Ni(n,γ)^{59}Ni reaction, and triggered by an AmBe neutron source, has been successfully built [129], yielding high γ-energies of 9 MeV. DUNE proposes to use a ^{252}Cf

(or AmLi as backup) neutron source with lower neutron energies, which requires less than half of the surrounding moderator, and making the ^{58}Ni (n, γ) source only 20 cm or less in diameter. The multipurpose instrumentation feedthroughs at either end of the cryostat are sufficient for this, and have an outer diameter of 25 cm. The moderator material chosen for DUNE is Delrin,[7] which has a large enough density to avoid flotation. Further, the end caps of the source body are round to avoid distorting the electric field and to eliminate the risk of the source getting stuck during deployment. Figure 6.26 depicts the primary source design of a cylindrical Delrin moderator with a diameter of 20 cm, a height of 40 cm including half-spheres at either end with radius of 10 cm, deployed at z=40 cm leaving a gap of 30 cm towards the FC and at a distance to the APA of x=220 cm, which is slightly further than mid-drift.

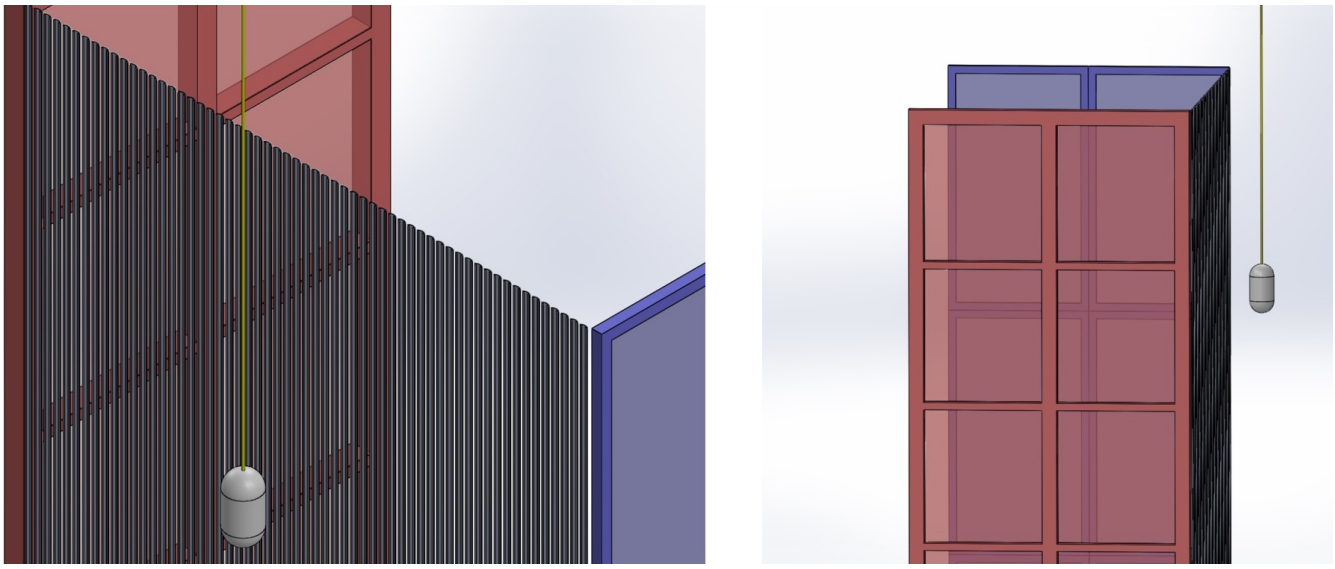

Figure 6.26: Fish-line deployment scheme in DUNE for a radioactive source encapsulated inside a cylindrical Delrin moderator body 20 cm in diameter and 40 cm high, including half-spheres with a radius of 10 cm at either end. A ^{252}Cf neutron source and a natural Ni target are sealed inside at the center. The fish-line is deployed 40 cm outside of the FC and 220 cm away from the APA (red plane).

A successfully employed multipurpose fish-line calibration system for the Double Chooz reactor neutrino experiment has become available after the decommissioning of Double Chooz in 2018. The system can be easily refitted for use in DUNE. The system will be housed inside a purge-box that is connected via a neck to a multipurpose calibration feedthrough with a closed gate valve on top of the cryostat. Before deployments, the source will be gently cooled-down by blowing liquid argon boil-off onto it inside a sealed purge-box. After the source has reached near-LAr temperatures, the purge-box will be evacuated by a vacuum pump to remove any residual oxygen and nitrogen which is monitored at the ppm level. Then, the entire purge-box interior is purged with boil-off liquid argon, and the pressure equalized with the gas pressure inside the detector, before the gate-valve is opened and deployments can commence. This procedure ensures that no significant impurities are introduced into the detector during a deployment and that no significant amount of liquid argon is boiled-off from the detector.

[7] DuPont™Delrin®, http://www.dupont.com/products-and-services/plastics-polymers-resins/thermoplastics/brands/delrin-acetal-resin.html.

Deployed near mid-drift (in each TPC module) the 9 MeV γ-ray source can illuminate the full drift length from APA to CPA. The sources are retrieved from the detector after each deployment and stored outside the cryostat following approved safety protocols, and the gate-valves are kept closed after deployments. More details on radiation safety and handling procedures are presented in Section 6.7.3.9.

6.7.3.2 Development Plan

The major development plans for the radioactive source deployment system include the following.

- Continue development of relevant simulation tools including geometry representation of the source deployment system and impact from various radiological contaminants on detector response.
- Conduct studies to suppress radiological backgrounds for the calibration source.
- Conduct simulation studies to understand data and trigger rates.
- Study a baseline design source with Delrin moderator, ^{252}Cf neutron source, and natural nickel target, both sealed inside at the moderator's center.
- Validate 9 MeV capture γ-ray yield of source using spectroscopic measurements with the 'RABBIT' germanium detector at South Dakota School of Mines and Technology (SDSMT), that has an assay chamber large enough to fit the bulky moderator.
- Validate with ^{3}He based hodoscope at SDSMT to ensure that the flux of neutrons escaping the moderator is not an issue; otherwise use lower energetic AmLi neutron source instead and/or more moderator material, and/or different geometric configuration of nickel target.
- Test gentle GAr cooling of source and validate material integrity. Measure tensile strength of braided SS-304 wire-rope at cryogenic temperatures and ensure a safety factor of one order of magnitude by adjusting number of steel braids and their diameters. Validate cryogenic shrinkage of sectional teflon sleeves, that enclose the braided steel wire-rope and electrically insulate it towards the FC.
- Validate that anticipated fluid flow in LAr does not cause oscillations of the source; otherwise design vertical guide wires to be pre-installed during detector installation which will keep source in stable position during deployment along the vertical axis.
- Explore other radioactive sources beyond the primary 9 MeV γ-ray nickel source, such as the previously mentioned 15 MeV γ-ray source based on the ^{40}Ar(α, γ)^{44}Ca process with ^{241}Am as the alpha emitter. This is currently being assembled at SDSMT. Furthermore, investigate hybrid neutron sources (^{252}Cf and AmBe) that emulate the kinetic neutron energy spectrum of radiological neutrons and probe the neutron tagging efficiency.

A successful demonstration of the RSDS in ProtoDUNE-2 running is the main priority for this system towards making a decision on deploying this system for the FD. A schedule with main steps towards ProtoDUNE-2 deployment is shown in Table 6.11.

Table 6.11: Key milestones towards commissioning the radioactive source deployment system in ProtoDUNE-2.

Milestone	Date (Month YYYY)
Baseline RSDS design validation	January 2020
RSDS mock-up deployment test at SDSMT	March 2020
RSDS Design review	May 2020
RSDS Production readiness review (PRR)	July 2020
Start of module 0 RSDS component production for ProtoDUNE-2	September 2020
End of module 0 RSDS component production for ProtoDUNE-2	February 2021
Start of ProtoDUNE-2 (SP) installation	**March 2021**
Start of RSDS installation	April 2021
RSDS demonstration test at ProtoDUNE-2	April 2022

6.7.3.3 Measurement Program

The proposed primary 9 MeV single γ source may also be used to test the γ component of the SNB and ^{8}B/hep solar neutrino signal along the full drift but only in the endwall regions of the detector. The source may also be used to determine the relative charge and light extraction efficiency in the vertical direction for measurements of energy resolution and energy scale.

Figure 6.27 depicts in a top view of the detector the simulated charge extraction efficiency for the 9 MeV γ-ray source deployed 40 cm outside of the FC, near mid-drift i.e., 220 cm away from the APA in the x direction, in the presence of expected background before (a) and after (b) applying selection cuts. The selection cuts are based on the amplitude and location of wire hits, and require a coincidence with a suitable signal in the PD system. Figure 6.27(b) shows that the selection cuts can reject radiological backgrounds almost entirely, and that the RSDS should allow the study of the trigger efficiency for isolated solar neutrino events, and its threshold dependence.

Figure 6.28 shows exemplary simulated RSDS measurements of the E field strength (a) and of the electron lifetime (b), each for three different scenarios. The analysis is based on fitting the measured distribution of drift-time, i.e., the time difference between the PD system signal and the recorded hit times on collection wires, passing the selection cuts. Figure 6.28(a) illustrates that with this method the E field strength could be measured at $\sim 1\,\%$ precision at each vertical deployment position at the endwalls. Likewise, Figure 6.28(b) illustrates that the electron lifetime could be measured at about $\sim 10\,\%$ precision (possibly better at higher lifetimes) at each vertical deployment position at the endwalls.

Figure 6.28(c) illustrates that it is not convincingly possible to unambiguously measure both the electron lifetime and the electric field strength with a recorded charge spectrum (after selection cuts) alone, since both parameters simply shift the upper falling edge of the charge spectrum up or down. However, when combined with the drift-time measurement, the charge measurement would provide an additional constrain that could possibly break correlations.

Aside from the primary 9 MeV γ-ray nickel source, other sources could be deployed with the same

multi-purpose system, for example a ^{40}Ar(α, γ)^{44}Ca gamma-ray source, a ^{252}Cf and/or AmBe neutron source that probe the impact of various radiological backgrounds, like radon (α, γ) or radiological neutrons, or simply measure the neutron tagging efficiency, useful for improved calorimetry of beam neutrino interactions. In contrast to the nickel source, the 15 MeV (α, γ) could be deployed outside of the cryostat.

An external ProtoDUNE-2 deployment can demonstrate the feasibility of the non-invasive 15 MeV ^{40}Ar(α, γ)^{44}Ca γ-ray source despite the lack of overburden to shield cosmic rays. In contrast to cosmic muons, 15 MeV γ-ray induced hit clusters will start inside the detector volume, and are not tracks that begin at the detector edges. Thus, the RSDS calibration events could therefore be easily selected and the detected charge can be analyzed. The detected light, however, will be obscured from the high light level in each drift period from cosmic muons hitting ProtoDUNE.

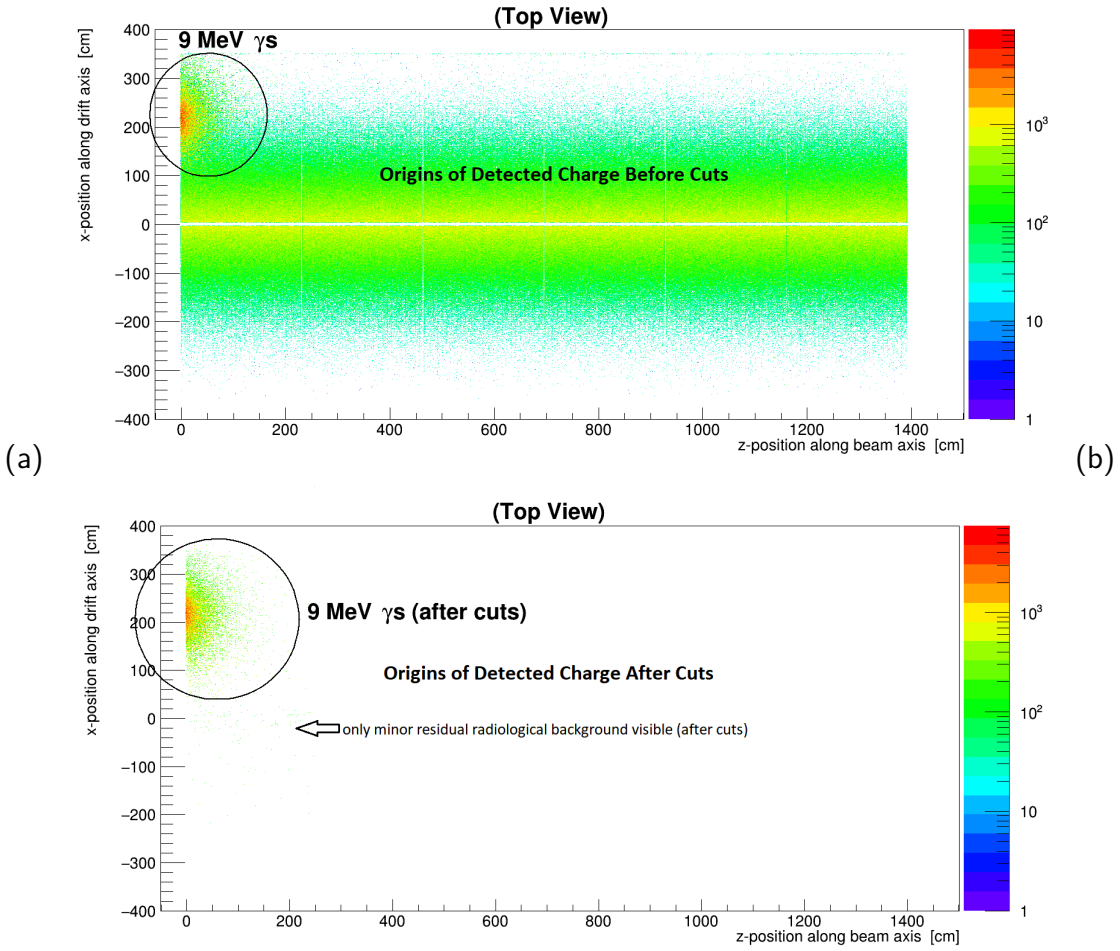

Figure 6.27: Detected charge (a) without cuts and (b) with selection cuts for a simulated 9 MeV γ-ray source deployed at z =−40 cm outside of the FC, x =220 cm away from the APA, and y =300 cm half-height of an upper endwall APA with simulated expected radiological background, that gets almost eliminated by selection cuts.

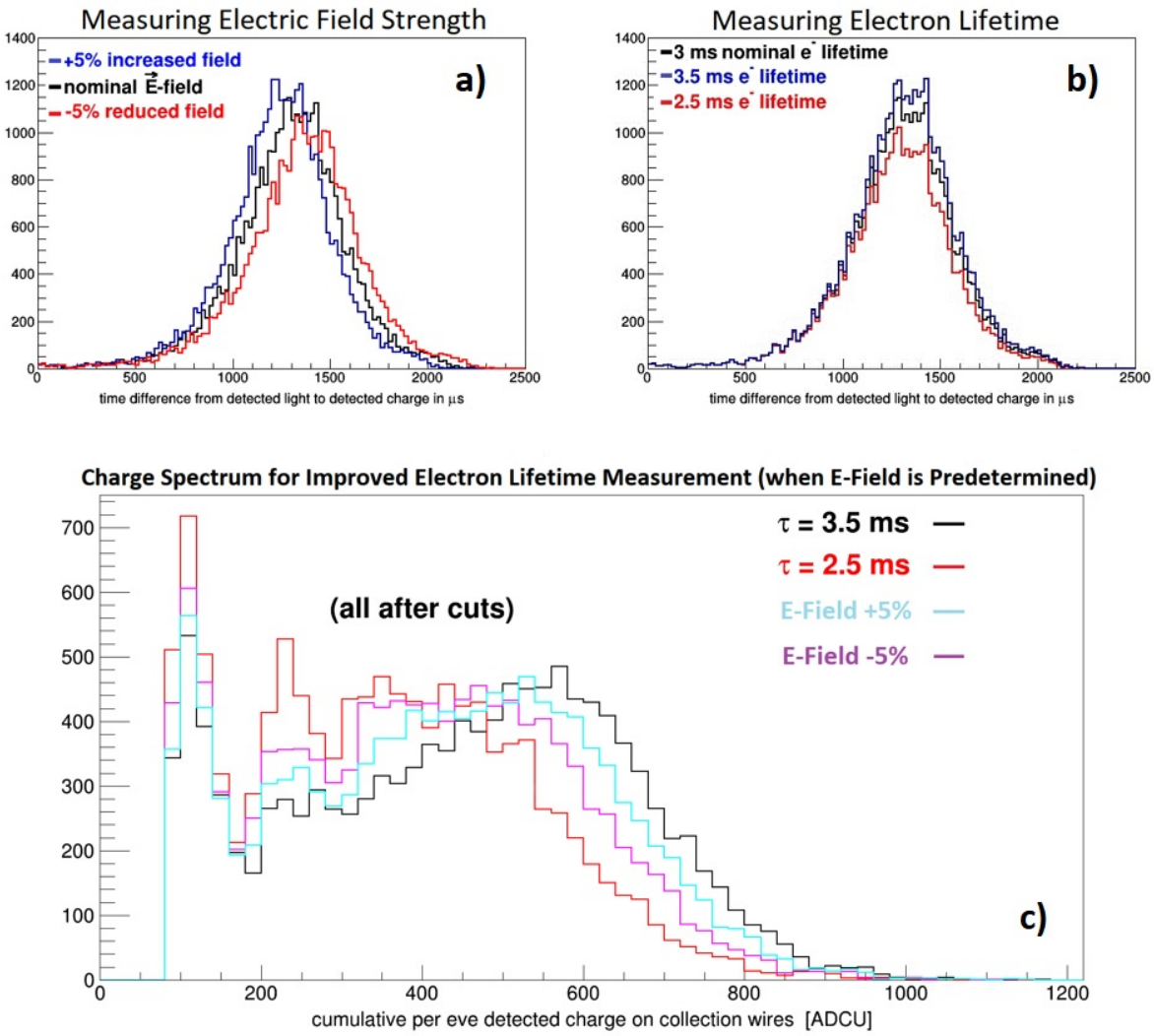

Figure 6.28: Simulated measurements of (a) E field strength from drift-time distribution, (b) electron lifetime from drift-time distribution, and (c) electron lifetime from charge distribution when electric field is unambiguously known from drift-time distribution. All spectra were created with applied selection cuts for a simulated 9 MeV γ-ray source with radiological backgrounds deployed at $z = -40$ cm outside of the FC, $x = 220$ cm away from the APA, and $y = 300$ cm half-height of an upper endwall APA. (Colors of histograms are matching colors of corresponding labels in each histogram.)

6.7.3.4 RSDS Design Validation

The cosmic induced background rate at ProtoDUNE is too high at the surface to detect responses to the DUNE γ-ray source; a higher intensity source could be deployed to test the detector response and analysis method. However, tests of functionality, reliability, and safety of the mechanical deployment system are essential to show the source can be deployed and retrieved with no issues, so these will be the main goals of the ProtoDUNE-2 deployment. As mentioned earlier, tests of the source design itself, in terms of γ activity, will be done at SDSMT.

6.7.3.5 DAQ Requirements

Section 6.4.1 provides an overall discussion of the Calibration and DAQ interface. Here, the DAQ requirements for the radioactive source deployment system are discussed. The radioactive source will not be triggerable by the MLT. Rather, it will deliver a tag to the MLT and that tag will include a time stamp that can be used by the MLT to issue a trigger command to the FE readout. The trigger command will have a standard readout window size of 5.4 ms, but to keep data rates manageable, the command will only be send to FE readout buffers that are expected to be illuminated by the source. The localization of trigger commands thus reduces the data volume by 150, if only one APA is read out.

Nevertheless, if the rate of such a source is anywhere close to one per 5.4 ms, the detector would be running continuously in the current scheme. Therefore we assume that the interaction rate in the detector is 10 Hz or less. The tag from the source will likely be much higher than this, because not all γs interact in the active TPC volume. Thus the radioactive source trigger will be a coincidence in the Module-Level Trigger between a low-energy trigger candidate from the illuminated APA, and a source tag with a relevant time stamp. With this rate, and with localization of events to one APA, the total data volume would be

$$8 \text{ hours} \times 4 \text{ FTs} \times 10\,\text{Hz} \times 1.5 \text{ Bytes} \times 2\,\text{MHz} \times 5.4\,\text{ms} \times 2560 \text{ channels} = 50\,\text{TB}/scan. \quad (6.4)$$

Running this calibration four times/year would yield 200 TB of data in 10 kt per year. Table 6.12 summarizes the data volume requirements for RSDS.

Table 6.12: Estimated data volume per year per 10 kt for the radioactive source system.

System	Data Volume ($\text{TB} \cdot \text{year}^{-1}$)	Assumptions
Proposed Radioactive Source System	200	Source rate $<$ 10 Hz; single APA readout, lossless readout; 4 times/year

6.7.3.6 Risks

The risks associated with the radioactive source system are described in Table 6.13 along with appropriate mitigation strategies and the impact (low, medium or high risk levels) on probability,

cost, and schedule post-mitigation. There are three residual medium-level risks in the table, more discussion on them is provided below:

- *Radioactivity leak:* If radioactivity leaks into the detector during a deployment, radiological backgrounds in the detector might increase. Rigorous source certification under high pressure and cryogenic temperatures mitigates this risk.
- *Source stuck or lost:* If the source gets stuck or is lost in the detector, then it becomes a permanent localized radiological background source. Fish-line an order of magnitude stronger than needed to hold the weight, round edges of the moderator and a torque limit of the stepper motor will mitigate this risk.
- *Oxygen and nitrogen contamination:* If the purge-box has a small leak, oxygen and nitrogen could get into the LAr. Leak checks before deployments will mitigate this risk.

Table 6.13: Radioactive source calibration system risks (P=probability, C=cost, S=schedule) The risk probability, after taking into account the planned mitigation activities, is ranked as L (low $<10\,\%$), M (medium $10\,\%$ to $25\,\%$), or H (high $>25\,\%$). The cost and schedule impacts are ranked as L (cost increase $<5\,\%$, schedule delay <2 months), M ($5\,\%$ to $25\,\%$ and 2–6 months, respectively) and H ($>20\,\%$ and >2 months, respectively).

ID	Risk	Mitigation	P	C	S
RT-SP-CAL-10	Radioactive source swings into detector elements	Constrain the system with guide-wires	L	L	L
RT-SP-CAL-11	Radioactivity leak	Obtain rigorous source certification under high pressure and cryogenic temperatures	L	L	M
RT-SP-CAL-12	Source stuck or lost	Safe engineering margins, stronger fish-line and a torque limit in deploy-ment system	L	M	L
RT-SP-CAL-13	Oxygen and nitrogen contamination	Leak checks before deployments	L	M	M
RT-SP-CAL-14	Light leak into the de-tector through purge-box	Light-tight purge box with an in-frared camera for visual checks	L	L	L
RT-SP-CAL-15	Activation of the cryo-stat insulation	Activation studies and simulations	L	L	L

6.7.3.7 Installation, Integration, and Commissioning

The first elements of the radioactive source guide system are installed before the TPC elements on the end wall farthest from the TCO and as the last system, concurrent and coordinated with the alternative laser system (if any deployed), once the TPC is installed before closing the TCO. The radioactive source deployment system is installed at the top of the cryostat and can be installed when DUNE becomes operational.

The commissioning plan for the source deployment system will include a dummy source deployment

(within 2 months of the commissioning) followed by first real source deployment (within 3 to 4 months of the commissioning) and a second real source deployment (within 6 months of the commissioning). Assuming stable detector conditions, the radioactive source will be deployed every half a year. Ideally, a deployment before and after a run period are desired so at least two data points are available for calibration. This also provides a check if the state of the system has changed before and after the physics data run. It is estimated that it will take a few hours (e.g. 8 hours) to deploy the system at one feedthrough location and a full radioactive source calibration campaign might take a week.

6.7.3.8 Quality Control

A mechanical test of the Double Chooz fish-line deployment system with a LAr mock-up column will be done in the high bay laboratory at SDSMT. The ultimate test of the system will be done at ProtoDUNE. Safety checks will also be done for the source and for appropriate storage on the surface and underground.

6.7.3.9 Safety

A composite source is used for the radioactive source system that consists of ^{252}Cf, a strong neutron emitter, and ^{58}Ni, which, via the ^{58}Ni(n,γ)^{59}Ni process, converts one of the ^{252}Cf fission neutrons, suitably moderated, to a monoenergetic 9 MeV gamma. This system also poses a radiation risk, which will be mitigated with a purge-box for handling, and a shielded storage box and an area with lockout-tagout procedures, also applied to the gate-valve on top of the cryostat. Material safety data sheets will be submitted to DUNE ES&H and specific procedures will be developed for storage and handling of sources to meet Fermilab Radiological Control Manual (FRCM) requirements. These procedures will be reviewed and approved by SURF and Fermilab radiation safety officers. Sources that get deployed will be checked monthly to ensure they are not leaking. A designated shielded storage area will be assigned for sources and proper handling procedures will be reviewed periodically. A custodian will be assigned to each shielded source.